DOKUZ EYLUL UNIVERSITY

GRADUATE SCHOOL OF NATURAL AND APPLIED SCIENCES

CO-DEPOSITION OF METAL FILMS WITH CERAMIC NANOPARTICLES ON METALLIC SUBSTRATES BY ELECTRODEPOSITION SYSTEM

by

Orkut SANCAKOĞLU

July, 2009

İZMİR

CO-DEPOSITION OF METAL FILMS WITH CERAMIC NANOPARTICLES ON METALLIC SUBSTRATES BY ELECTRODEPOSITION SYSTEM

A Thesis Submitted to the

Graduate School of Natural and Applied Sciences of Dokuz Eylul University

In Partial Fulfillment of the Requirements for the Degree of

Master of Science in Metallurgical and Materials Engineering,

Metallurgical and Materials Program

by

Orkut SANCAKOĞLU

July, 2009

İZMİR

M. Sc. THESIS EXAMINATION RESULT FORM

We have read the thesis entitled **"CO-DEPOSITION OF METAL FILMS WITH CERAMIC NANOPARTICLES ON METALLIC SUBSTRATES BY ELECTRODEPOSITION SYSTEM"** completed by **ORKUT SANCAKOGLU** under revision of **ASSOC. PROF. DR. ERDAL ÇELİK** and we certify that in our opinion it is fully adequate, in scope and in quality, as a thesis for the degree of Master of Science.

.....

Assoc. Prof. Dr. Erdal ÇELİK

Supervisor

.....

(Jury Member)

.....

(Jury Member)

Prof. Dr. Cahit HELVACI

Director

Graduate School of Natural and Applied Science

ACKNOWLEDGEMENTS

I sincerely thank for the people who mentally support and encourage me, aid me in my pursuing of the M. Sc. degree, and help in my academic accomplishment.

I cordially would like to express my thanks to my supervisor, Assoc. Prof. Dr. Erdal ÇELİK for his guidance, interest and encouragement.

I also would like to thank my all colleagues especially Elif Zehra EROĞLU and Mustafa EROL for their cooperation and friendship.

Finally, I would like to thank my family for their support and persistence.

I also would like to thank The Scientific and Technological Research Council of Turkey (TUBITAK) for financial support in my master degree period. And the present study was also supported by Ministry of Industry and Trade with the project code 0099-STZ-2007-1.

Orkut SANCAKOĞLU

CO-DEPOSITION OF METAL FILMS WITH CERAMIC NANOPARTICLES ON METALLIC SUBSTRATES BY ELECTRODEPOSITION SYSTEM

ABSTRACT

In this research; submicron sized ceramic particles alumina, silicon carbide and tungsten carbide were co-deposited with metals zinc and chromium via electrodeposition system to fabricate zinc-alumina, chromium-silicon carbide and chromium-tungsten carbide metal matrix composite structures. With this aim, new systems were designed instead of traditional electrodeposition cells and coatings were fabricated in these systems for different electrolyte compositions. These composite coatings were produced under different combinations of system parameters such as current density, pH, temperature, current type and frequency which effect co-deposition directly.

Phase identifications of the fabricated composite coatings were performed by Shimadzu-6000 model XRD (X-ray diffractometer) and surface morphologies were investigated using JEOL-JJM 6060 model SEM (scanning electron microscopy) with an EDS (energy dispersive X-ray spectroscopy) system attachment. Nevertheless, mechanical properties of the coatings such as hardness, elastic modulus and elastic recovery rate percentages were performed under 25 mN applied load by Shimadzu DUH-W201, DUH-W201S model Dynamic Micro-Hardness Tester with a working range 0,1 – 1961 mN and under 980,7 mN applied load using Shimadzu HMV-2 model Micro-Hardness Tester with a working range 98,07 mN (HV0.1) - 19.614 N (HV2). It was concluded that ceramic particles alumina/silicon carbide/tungsten carbide were physically absorbed to the cathode surface and made a composite structure with metal Zn/Cr and co-deposition of sub-micron sized ceramic particles with metals via electrodeposition system was strictly successful.

Keywords: Electrodeposition, co-deposition technique, MMCs (metal matrix composites), Dynamic Micro-Hardness Test (DUH).

METAL FİLMLERİN SERAMİK NANOPARTİKÜLLERLE BİRLİKTE ELEKTROKİMYASAL YÖNTEMLE METALİK ALTLIKLAR ÜZERİNE DEPOZİTLENMESİ

ÖZ

Bu çalışmada; çinko ve krom metalleri ile mikron-altı boyutta alümina, silisyum karbür ve tungsten karbür seramik partikülleri, elektrokimyasal yöntemle birlikte depozitlenerek çinko-alümina, krom-silisyum karbür ve krom-tungsten karbür metal matrisli kompozit yapıları oluşturulmuştur. Burada; geleneksel elektrokimyasal hücre yerine, yeni sistemler tasarlanmıştır ve kaplamalar çeşitli elektrolit kompozisyonları için bu sistemlerde üretilmiştir. Sözü edilen kompozit kaplamalar; akım yoğunluğu, pH, sıcaklık, karıştırma tipi, akım tipi ve frekans gibi birlikte depozitlemeyi etkileyen sistem parametrelerinin çeşitli kombinasyonları için üretilmiştir.

Üretilen kompozit yapıların faz ve morfolojik yapıları, elementsel haritalama sonuçları gibi nitel ve nicel karakterizayson işlemleri, Shimadzu-6000 model XRD (X-ışınları difraktometresi) SEI ve BEI olmak üzere iki farklı modda görüntü alabilen, EDS (enerji saçınım spektrometresi) entegreli JEOL-JJM 6060 model SEM (taramalı elektron mikroskobu) cihazlarında incelenmiştir. Bunun yanında kompozit yapılara ait sertlik, elastisite modülü ve elastik toparlanma yüzdeleri gibi mekanik özellikler 0,1 - 1961 mN yük aralığında çalışabilen Shimadzu DUH-W201, DUH-W201S model Dinamik Mikro-Sertlik Test cihazında, 25 mN yük altında ve 98,07 mN (HV0.1) - 19.614 N (HV2) çalışma aralığı kapasiteli Shimadzu HMV-2 model Mikro-Sertlik Test cihazında 980,7 mN yük altında belirlenmiştir. Sonuç olarak bu çalışma, alümina/silisyum karbür/tungsten karbür gibi seramik partiküllerin katot yüzeyinde fiziksel olarak absorblanarak Zn/Cr gibi metallerle kompozit yapılar oluşturduğunu ve metallerle mikron-altı boyuttaki seramik partiküllerin elektrodepozitleme sistemi ile başarılı bir şekilde depozitlendiğini göstermiştir.

Anahtar kelimeler: Elektrodepozitleme, Birlikte depozitleme tekniği, Metal matrisli kompozitler, Dinamik mikro-sertlik.

CONTENTS

Page

CHAPTER ONE
INTRODUCTION AND MOTIVATION

In most cases, materials have a limited lifetime, which depends strongly on the action of external factors and the operating environment. There are usually mechanical interactions between components in contact with one another. Occasionally, there will be chemical or electrochemical reactions with the environment, which will sooner or later damage functionality by attacking the surface. The surface of a material or component might be deemed, because of its atomic structure, to be the most vulnerable site for various forms of attack. This could be mechanical, chemical, electrochemical or thermal in nature. The effects could be present individually or in combination. There are lots of coating techniques such as; vapor deposition, painting, thermal spray, galvanizing and so on to maximize the lifetime of the materials (Kanani, 2004, p.2).

In addition to the coating processes detailed above, electrodeposition of metals, as a surface coating technology, has special importance (Kanani, 2004, p.3). Among the processes, in order to produce nanostructured composites, the electrodeposition technique has further demonstrated that a smoother surface, a better bonding between particles and metal, easy to control the thickness of the coating, appropriate to automation, available for obtaining metallic alloys and composite coatings and higher microhardness can be achieved (Ciubotariu et al., 2008). Anti-corrosion coatings, especially zinc have been widely investigated in this technique. Compared to other metals, zinc is anodic to iron and steel and therefore offers more protection if applied in thin films than similar thicknesses of nickel and other cathodic coatings. It is relatively inexpensive than other metals and readily applied in barrel, tank or continuous plating facilities (ASM-International Handbook Committee [IHC], 1994, p.804). And also chromium is anodic when compared to other metals. For both chromium type of alloys and pure chromium coatings, the most important properties to develop in a coating are corrosion resistance, abrasion and wear resistance, hardness, surface texture, and luster. Thickness requirements can range from a few microns up to a few hundred microns.

Traditionally, researchers have been focused on the corrosion behaviors of the zinc and chromium coatings but not on mechanical properties. It is known that not only the corrosion properties but also the mechanical properties are important for industrial applications. Much recent attention has been focused on the development of techniques for electroplating alloys including zinc-iron (Thiemig et al., 2009), zinc-nickel (Hammami et al., 2009), zinc-cobalt (Chandrasekar et al., 2009), chromium-iron, chromium-nickel, and chromium-iron-nickel and electrodeposited hard metal coatings such as pure chromium (Lubnin, 2006). Different types of nanocomposites such as Ni-ZrO_2, Ni-SiC, Ni-PZT, Ni-Al_2O_3, Ni–diamond and Cu-Al_2O_3 have been successfully produced by direct current (DC), pulse current (PC) and pulse reverse current (PRC) electrodeposition (Benea, 1998, 2002).

There are not so much alternatives to obtain materials with both improved corrosive and mechanical properties. It is known that "combining the best properties of two different materials to obtain one material with excellent properties" is the main idea of fabricating composites. Based on the idea determined above, co-deposition technique is feasible to combine the excellent corrosive protection property of Zn/Cr and both the corrosive and mechanical properties of Al_2O_3/SiC/WC.

Co-deposition of metals with ceramic particles is a new technique to obtain hard and wear resistant coatings and it is not studied enough. The co-deposition of Al_2O_3 was also studied by Kuo et al.(2004) using pulse current and ultrasonic energy treatment. The corrosion properties of obtained composite coatings were not discussed. In addition, co-deposited composite coatings with a metal matrix and non-metallic inclusions have excellent wear resistance and permit emergency dry-running of machinery. To give some examples; nickel coatings with 8-10 % vol. of silicon carbide are used to increase the life of internal combustion engine cylinder bores, composite coatings based on chromium carbide in a cobalt matrix are used as wear-resistant coatings in gas turbines where they are required to perform for extended periods at temperatures of up to ~800^oC, chromium deposits with alumina inclusions are used in piston rings for diesel engines. Single crystal diamonds locked into a

nickel matrix form the cutting edge in tools such as chainsaws, grinding discs or dental drills (Kanani, 2004, p.11).

A number of workers have investigated the mechanism of the electrodeposition of composites, and most of their proposed mechanisms involve one or more of the following three processes (Kanani, 2004, p.110);

1. Electrophoretic movement of positively charged particles to the cathode,
2. Adsorption of the particles at the electrode surface by Van der Waals forces, and
3. Mechanical inclusion of the particles into the layer.

There are many models, which offer a quantitative relationship for the incorporation rate of the particles into the matrix, but the current and most known model is detailed above. The regions include: formation of ionic clouds around the particles (bulk electrolyte, typical length in cm); convective movement toward the cathode (convection layer, typical length <1 mm); diffusion through a concentration boundary layer (diffusion layer, typical dimensions of hundreds of μm); electrical double layer (typical dimensions of nm) followed by adsorption and entrapment of particles (Roos et al., 1990).

These steps mark the progress of particles from the bulk solution to their incorporation in the deposit. The first stage postulates formation of an electro-active ionic cloud surrounding the particle, as soon as these are introduced into the electrolyte. Under the action of convection, these ionically enveloped particles are transported to the hydrodynamic boundary layer, migrate across this and are conveyed by diffusion to the cathode. After the ionic cloud is wholly or partly reduced, the particles are deposited and incorporated in the matrix as the metal ions are discharged, so 'burying' the inert particles (Kanani, 2004, p.110).

With the shore of commentaries explained above, while some researchers focused on nickel (Leighton, 1994) and some other metals (Ramanauskas, 1997), and some of them focused on the static hardness (Bohe, 1991) and wear properties of these composite coatings (Gogotski, 1999), it was decided to study on the nano

indentation behaviors. These properties will make us to predict on the mechanical properties of the coatings like wear and microhardness.

Zn and chromium alloys have been widely applied as high corrosion (Leighton, 1994) and wear resistant coatings, respectively, in several industrial applications (Ramanauskas, 1997). Submicron sized Al_2O_3, SiC and WC have been used extensively in metal matrix composite coatings because of their high microharness (Bohe, 1991), wear resistance (Vilche, 1989) and excellent chemical stability (Gogotski, 1999). However, no report has been published on the fabrication of Zn–Al_2O_3 composite coatings and their nano indentation research and not enough study on co-deposition of hard chromium and sub-micron sized ceramic powders.

The aim of this thesis is to fabricate Zn-Al_2O_3, Cr-WC and Cr-SiC composite coatings with the aid of stirrer pomp, magnetic stirrer and air ventilation to suspense the ceramic particles in the electrolyte and consequently to characterize the coating morphologies and investigate the mechanical properties. Therefore, we draw attention to microstructural and mechanical properties of these composite coatings formed on brass/steel substrates by electro-deposition process. In this context, the coatings were by electro-deposition technique. The produced coatings were characterized by X-ray diffractometer (XRD), scanning electron microscope (SEM) including energy dispersive spectroscopy (EDS). Mechanical properties of the coatings were examined by Shimadzu Dynamic Ultra-micro Hardness/Micro Vickers Hardness Test Machines for estimating young's modulus due to load-unload sensing analysis, in addition to mechanical investigation hardness-depth and load-hardness curves of the layer was obtained to expose ceramic particle effect on mechanical properties in same conditions.

CHAPTER TWO
NANOCOMPOSITE SCIENCE AND TECHNOLOGY

2.1 General Aspect on Nanotechnology

Nanotechnology is engineering at the molecular (groups of atoms) level. It is the collective term for a range of technologies, techniques and processes that involve the manipulation of matter at the smallest scale (from 1 to 100 nanometres - 1/10,000th the thickness of a human hair).

At this very small scale, the properties of materials such as colour, magnetism and the ability to conduct electricity change in unexpected ways. This results in new, exciting and different characteristics that can generate a vast array of novel products.

Because nanotechnology is classified by the ***size of the materials*** being developed and used, the products of this engineering can have little in common with each other - for example fuel cells, fabrics or drug delivery devices. What brings them together is the natural convergence of all basic sciences (biology, physics and chemistry) at the molecular level.

Nanotechnology is not new. Nanoproducts are already in the marketplace, such as stainresistant and wrinkle-free textiles. But because it transcends the conventional boundaries between physics, chemistry, biology, mathematics, information technology, and engineering, nanotechnology has the potential to transform the way we live. Some of the ways in which nanoproducts are predicted to impact on everyday life are illustrated in the cartoon (Figure 2.1) below from the EU publication ***Nanotechnology: Innovation for tomorrow's world*** (Prime Minister's Science, Engineering and Innovation Council [PMSEIC], 2005, p.1).

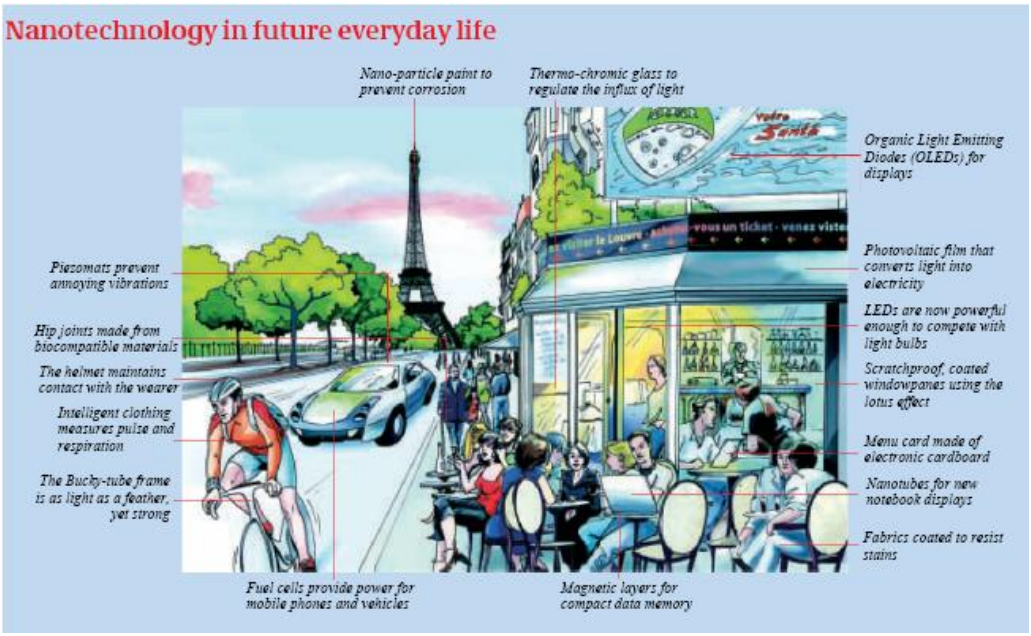

Figure 2.1 Several nanotechnological applications in future life (PMSEIC, 2005, p.2).

The disruptive innovations that should arise from nanotechnology over the next decade could be as significant as electricity or the microchip. They could give rise to a whole new set of industries as well as transform current technologies in manufacturing, healthcare, electronics and communications. It has been estimated that the sales of products incorporating emerging nanotechnologies will rise from 0.1% of global manufacturing output in 2004 to 15% in 2014, totalling US$2.6 trillion. This would be as large as information and communication technologies combined and more than ten times larger than biotechnology revenues.

Importantly, unlike information technology where, for example, consumers might buy a computer, nanotechnology consumers will not buy a ‘nanotechnology product’ but will buy a product developed or enhanced through nanotechnology.

Examples of exciting applications of nanotechnology include:

- *Nanopowders* - the unusual properties of particles less than 100 nm allow a range of new and improved materials with a breadth of applications, such as plastics that behave like ceramics or metals; new catalysts for environmental remediation; improved food shelf-life and packaging; and novel drug delivery devices.

- *Carbon nanotubes* - graphite can be rolled into a cylinder with a diameter of about 1 nm. These strong but light 'carbon nanotubes' are being developed for a raft of uses, such as sensors, fuel cells, computers and televisions.
- *Nanomembrane filtration systems* - these have the potential to address one of the most pressing issues of the 21st Century - safe, clean, affordable water.
- *Molecular electronic 'cross bar latches'* - Hewlett-Packard believes that silicon computer chips will probably reach a technical dead end in about a decade, to be replaced by tiny nanodevices described as 'cross bar latches'.
- *Quantum dots* - these are small devices that contain a tiny droplet of free electrons - essentially artificial atoms. The potential applications are enormous, such as counterfeit-resistant inks, new bio-sensors, quantum electronics, photonics and the possibility of tamper-proof data transmission.
- *New technologies for clean and efficient energy generation*.

The challenge for the next decade is to ensure that the full potential of this exciting technology can be harnessed, while ensuring that the social, ethical and safety issues are properly addressed (PMSEIC, 2005, p.3).

2.1.1 What is Nanotechnology?

The classical laws of physics and chemistry do not readily apply at this very small scale for two reasons. Firstly, the electronic properties of very small particles can be very different from their larger cousins. Secondly, the ratio of surface area to volume becomes much higher, and since the surface atoms are generally most reactive, the properties of a material change in unexpected ways. For example, when silver is turned into very small particles, it takes on anti-microbial properties while gold particles become any colour you choose.

Nature provides plenty of examples of materials with properties at the nanoscale – such as the iridescence of butterfly wings, the sleekness of dolphin skin or the 'nanofur' that allows geckos to walk up vertical surfaces. This latter example is illustrated in Figure 2.2. The Gecko foot pad is covered with aggregates of hair formed from nanofibres which impart strong adhesive properties.

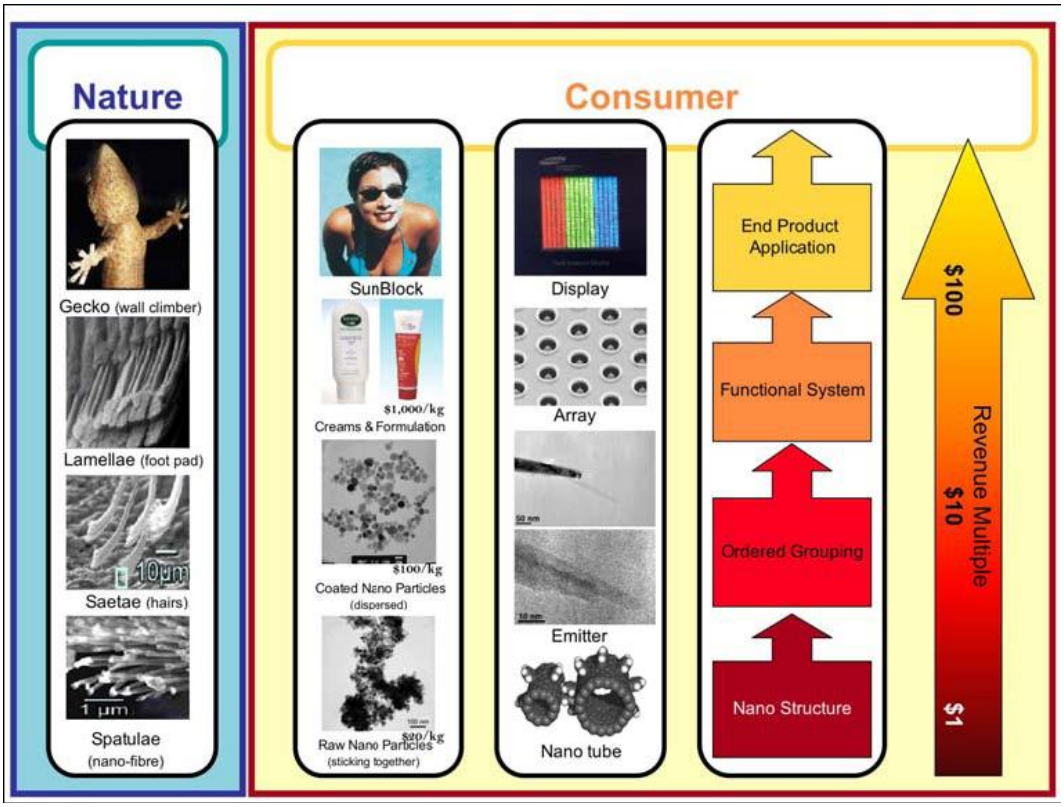

Figure 2.2 Examples of nanostructures in nature and nanotechnology (PMSEIC, 2005, p.8).

*One nanometre (1 nm) is defined as one billionth of a metre (10^{-9} m). This is the diameter of several atoms, and on the scale of individualmolecules. A human hair is approximately 80 000 nm wide, a red blood cell is 7000 nm wide, a DNA molecule is approximately 2 nm wide.

Nanotechnologists use similar principles to deliberately engineer at the nanoscale to create products that make use of these unusual properties. Starting with nanostructures, scientists rearrange them and then assemble functional systems that can be incorporated into products with unique properties. Figure 2.2 shows two examples. Firstly, the propensity for carbon to form tubes at the nanoscale can be used to generate arrays over micron sized conductors that illuminate flat panel displays for mobile phones, and secondly nanoparticles can be manipulated to create effective, fully transparent sunblock creams. These are but two of many examples of stronger, stickier, smoother and lighter products being developed.

2.1.2 Nanotechnology is a Set of Enabling Technologies

Nanotechnology is not confined to one industry, or market. Rather, it is an enabling set of technologies that cross all industry sectors and scientific disciplines. Probably uniquely, it is classified by the *size of the materials* being developed and

used, not by the processes being used or products being produced. Nanoscience is inherently multidisciplinary: it transcends the conventional boundaries between physics, chemistry, biology, mathematics, information technology, and engineering. This also means it can be hard to define – is the introduction of foreign genes or proteins into cells biotechnology or nanotechnology? And since genes have genetic memory, might this also be a form of information technology? The answer is probably 'all of the above'. The important point is that the integration of these technologies and their manipulation at the molecular and sub-molecular level will over the next decade provide major advances across many existing industries and create whole new industries.

2.1.3 Why is There so Much Interest in Nanotechnology?

Nanotechnology is not new - nanoproducts are already in the marketplace, such as stainresistant and wrinkle-free textiles. Given its fuzzy definition, there is also an element of rebadging traditional products under the nanotechnology banner.

However, because nanotechnology is ubiquitous but also far-reaching, it has real potential to transform the way we live. There are very significant economic, social and environmental implications from this technology. To quote *The Economist* (January 2005): 'Nanotechnology will indeed affect every industry through improvements to existing materials and products, as well as allowing the creation of entirely new materials' and 'produce important advances in areas such as electronics, energy and biomedicine' (PMSEIC, 2005, chap.1).

2.1.4 Why is Nanotechnology Important to Turkiye?

Global developments in nanotechnology will certainly impact on many of Turkiye's most important traditional industry sectors, and will raise social and safety issues that must be addressed. Nanotechnology capability is growing across a number of industry sectors in Turkiye, including minerals, agribusiness, health and medical devices, and energy and environment.

2.2 What's Happening Globally?

2.2.1 Brief History of Nanotechnology

Nanoparticles of gold and silver have been found in Ming dynasty pottery and stained glass windows in medieval churches. However, the origins of nanotechnology did not occur until 1959, when Richard Feynman, US physicist and Nobel Prize winner, presented a talk to the American Physical Society annual meeting entitled ***There's Plenty of Room at the Bottom***. In his talk, Feynman presented ideas for creating nanoscale machines to manipulate, control and image matter at the atomic scale. In 1974, Norio Taniguchi introduced the term 'nanotechnology' to represent extra-high precision and ultra-fine dimensions, and also predicted improvements in integrated circuits, optoelectronic devices, mechanical devices and computer memory devices. This is the so called 'top-down approach' of carving small things from large structures. In 1986, K. Eric Drexler in his book *Engines of Creation* discussed the future of nanotechnology, particularly the creation of larger objects from their atomic and molecular components, the so called 'bottom-up approach'. He proposed ideas for 'molecular nanotechnology' which is the self assembly of molecules into an ordered and functional structure.

The invention of the scanning tunneling microscope by Gerd Binnig and Heinrich Rohrer in 1981 (IBM Zurich Laboratories), provided the real breakthrough and the opportunity to manipulate and image structures at the nanoscale. Subsequently, the atomic force microscope was invented in 1986, allowing imaging of structures at the atomic scale. Another major breakthrough in the field of nanotechnology occurred in 1985 when Harry Kroto, Robert Curl and Richard Smalley invented a new form of carbon called fullerenes ('buckyballs'), a single molecule of 60 carbon atoms arranged in the shape of a soccer ball. This led to a Nobel Prize in Chemistry in 1996.

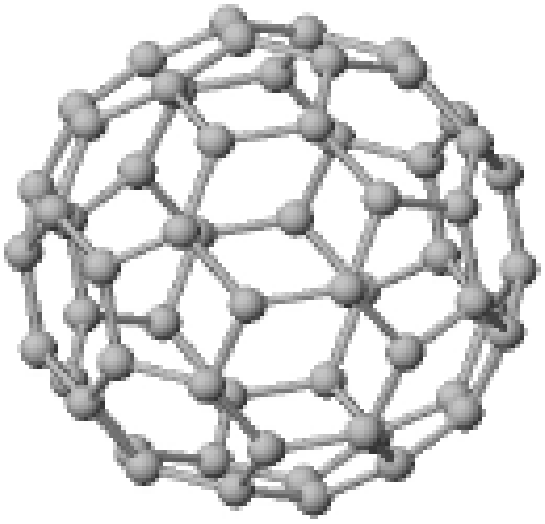

Figure 2.3 C_{60} image from the Sussex Fullerene Research Centre (PMSEIC, 2005, p.12).

Since that time, nanotechnology has evolved into one of the most promising fields of science, with multi-billion dollar investments from the public and private sectors and the potential to create multi-trillion dollar industries in the coming decade.

2.2.2 Unifying Themes of Nanotechnology

Because nanotechnology is classified by the *size of the materials* being developed and used, the products of this engineering can have little in common with each other – for example fuel cells, fabrics or drug delivery devices. What brings them together is the natural convergence of all basic sciences (biology, physics, and chemistry) at the molecular level. At this level, these diverse fields are unified by the following common themes:

1. *Characterisation tools* — to be able to examine and see the nanostructures or the building blocks of nanomaterials, characterisation tools such as X-ray diffraction, Synchrotron, Scanning and Transmission Electron Microscopy, Scanning Tunneling and Atomic Force Microscopy are powerful tools across disciplines.

2. *Nanoscale science* — because the properties of materials change in unexpected ways at the nanoscale, the science of understanding the behavior of molecules at this

scale is critical to the rational design and control of nanostructures for all product applications.

3. *Molecular level computations* — computation technologies such as quantum mechanical calculations, molecular simulations and statistical mechanics are essential to the understanding of all nanoscale phenomena and molecular interactions.

4. *Fabrication and processing technology* — many nanoparticles, powders and suspensions can be directly applied in paints, cosmetics, and therapeutics.

However, other nanomaterials must be assembled and fabricated into components and devices. In addition, processing techniques such as sol-gel, chemical vapor deposition, hydrothermal treatment, ***electrodeposition*** and milling are common techniques.

2.2.3 Examples of Nanotechnology

Nanopowders contain particles less than 100 nm in size - 1/10,000th the thickness of a human hair. The physical, chemical and biological properties of such small particles allow industry to incorporate enhanced functionalities into products.

Some of the unique properties of interest to industry are enhanced transparency from particles being smaller than the wavelength of visible light, and high surface areas for enhanced performance in surface area-driven reactions such as catalysts and drug solubilisation.

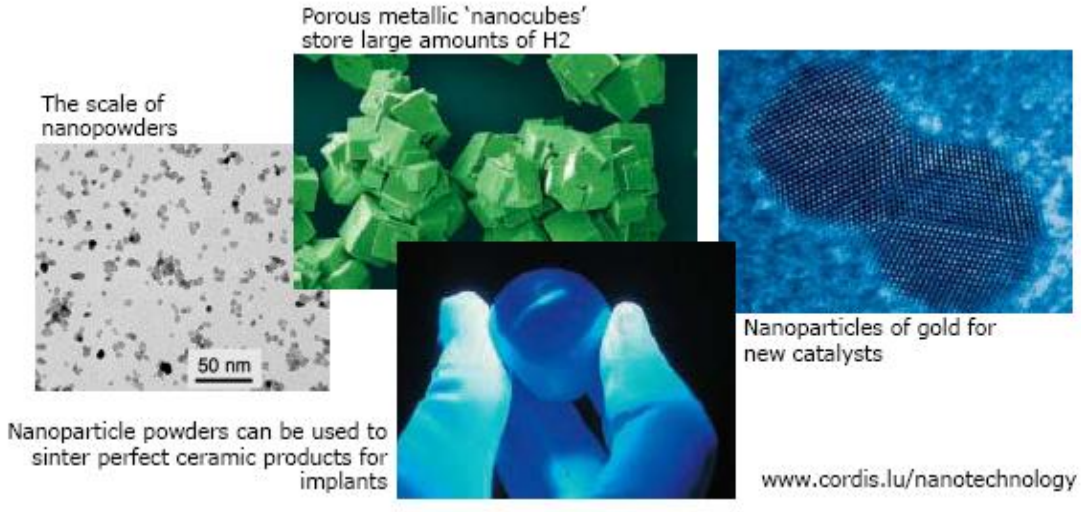

Figure 2.4 Present applications in nanotechnology (PMSEIC, 2005, p.13).

These unique properties give rise to a range of new and improved materials with a breadth of applications. To illustrate, nanotechnology allows plastics to retain transparency while also taking on characteristics such as resistance to abrasion, conductivity or UV protection found in ceramics or metals. New medical nanomaterials are being developed, such as synthetic bone and bone cement, as well as drugs with improved solubility to allow lower dosing, more efficient drug delivery and fewer adverse side effects (PMSEIC, 2005, p.13).

The high surface areas of nanoparticles are being exploited by industry in catalysts that improve chemical reactions in applications such as cleaning up car exhausts and potentially to remove toxins from the environment. For instance, petroleum and chemical processing companies are using nanostructured catalysts to remove pollutants - $30 billion industry in 1999 with the potential of $100 billion per year by 2015. Improved catalysts illustrate that improvements to existing technology can open up whole new markets – nanostructured catalysts look likely to be a critical component in finally making fuel cells a reality, which could transform our power generation and distribution industry (PMSEIC, 2005, p.14).

2.3 Nanocomposite Science and Technology

The field of nanocomposite materials has had the attention, imagination, and close scrutiny of scientists and engineers in recent years. This scrutiny results from the simple premise that using building blocks with dimensions in the nanosize range makes it possible to design and create new materials with unprecedented flexibility and improvements in their physical properties. This ability to tailor composites by using nanosize building blocks of heterogeneous chemical species has been demonstrated in several interdisciplinary fields. The most convincing examples of such designs are naturally occurring structures such as bone, which is a hierarchical nanocomposite built from ceramic tablets and organic binders. In as much as the constituents of a nanocomposite have different structures and compositions and hence properties, they serve various functions. Thus, the materials built from them can be multifunctional. Taking some clues from nature and based on the demands that emerging technologies put on building new materials that can satisfy several functions at the same time for many applications, scientists have been devising synthetic strategies for producing nanocomposites. These strategies have clear advantages over those used to produce homogeneous large-grained materials. Behind the push for nanocomposites is the fact that they offer useful new properties compared to conventional materials.

The concept of enhancing properties and improving characteristics of materials through the creation of multiple-phase nanocomposites is not recent. Nanocomposites can be considered solid structures with nanometer-scale dimensional repeat distances between the different phases that constitute the structure. These materials typically consist of an inorganic (host) solid containing an organic component or vice versa. Or they can consist of two or more inorganic/organic phases in some combinatorial form with the constraint that at least one of the phases or features be in the nanosize. Extreme examples of nanocomposites can be porous media, colloids, gels, and copolymers. In this chapter, however, we focus on the core concept of nanocomposite materials, i.e., a combination of nano-dimensional phases with distinct differences in structure, chemistry, and properties. One could think of the nanostructured phases present in

nanocomposites as zero-dimensional (e.g., embedded clusters), 1D (one-dimensional; e.g., nanotubes), 2D (nanoscale coatings), and 3D (embedded networks). In general, nanocomposite materials can demonstrate different mechanical, electrical, optical, electrochemical, catalytic, and structural properties than those of each individual component. The multifunctional behavior for any specific property of the material is often more than the sum of the individual components.

Both simple and complex approaches to creating nanocomposite structures exist. A practical dual-phase nanocomposite system, such as supported catalysts used in heterogeneous catalysis (metal nanoparticles placed on ceramic supports), can be prepared simply by evaporation of metal onto chosen substrates or dispersal through solvent chemistry. On the other hand, material such as bone, which has a complex hierarchical structure with coexisting ceramic and polymeric phases, is difficult to duplicate entirely by existing synthesis techniques. The methods used in the preparation of nanocomposites range from chemical means to vapor phase deposition.

Apart from the properties of individual components in a nanocomposite, interfaces play an important role in enhancing or limiting the overall properties of the system. Due to the high surface area of nanostructures, nanocomposites present many interfaces between the constituent intermixed phases. Special properties of nanocomposite materials often arise from interaction of its phases at the interfaces. An excellent example of this phenomenon is the mechanical behavior of nanotube-filled polymer composites. Although adding nanotubes could conceivably improve the strength of polymers due to the superior mechanical properties of the nanotubes, a noninteracting interface serves only to create weak regions in the composite, resulting in no enhancement of its mechanical properties.

2.3.1 Ceramic/Metal Nanocomposites

Many efforts are under way to develop high-performance ceramics that have promise for engineering applications such as highly efficient gas turbines, aerospace materials, automobiles, etc. Even the best processed ceramic materials used in

applications pose many unsolved problems; among them, relatively low fracture toughness and strength, degradation of mechanical properties at high temperatures, and poor resistance to creep, fatigue, and thermal shock. Attempts to solve these problems have involved incorporating second phases such as particulates, platelets, whiskers, and fibers in the micron-size range at the matrix grain boundaries. Nonetheless, results have been generally disappointing when micron-size fillers are used to achieve these goals.

Recently the concept of nanocomposites has been considered, which is based on passive control of the microstructures by incorporating nanometer-size second-phase dispersions into ceramic matrices (Ajayan et al., 2003, p.2). The dispersions can be characterized as either intragranular or intergranular as shown in Figure 2.5. These materials can be produced by incorporating a very small amount of additive into a ceramic matrix. The additive segregates at the grain boundary with a gradient concentration or precipitates as molecular or cluster sized particles within the grains or at the grain boundaries. Optimized processing can lead to excellent structural control at the molecular level in most nanocomposite materials. Intragranular dispersions aim to generate and fix dislocations during the processing, annealing, cooling, and/or the in-situ control of size and shape of matrix grains. This role of dispersoids, especially on the nano scale, is important in oxide ceramics, some of which become ductile at high temperatures. The intergranular nanodispersoids must play important roles in control of the grain boundary structure of oxide (Al_2O_3, MgO) and nonoxide (Si_3N_4, SiC) ceramics, which improves their high-temperature mechanical properties. The design concept of nanocomposites can be applied to ceramic/metal, metal/ceramic, and polymer/ceramic composite systems.

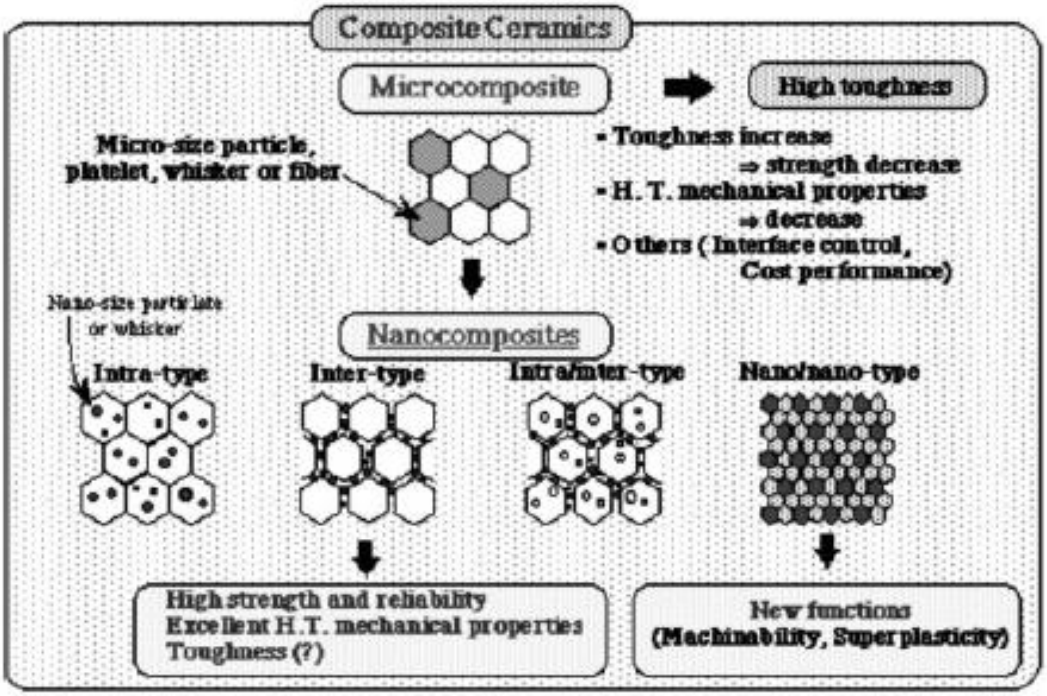

Figure 2.5 New concepts of ceramic metal nanocomposites with inter- and intra-granular designs: properties of ceramic materials can be improved by nanocomposite technology (Ajayan et al., 2003, p.3)

2.3.2 Metal Matrix Nanocomposites

During the past decade, considerable research effort has been directed towards the development of in situ metal-matrix composites (MMCs), in which the reinforcements are formed by exothermal reactions between elements or between elements and compounds. With this approach, MMCs with a wide range of matrix materials (including aluminum, titanium, copper, nickel, and iron), and second-phase particles (including borides, carbides, nitrides, oxides, and their mixtures) have been produced. Because of the formation of stable nanosized ceramic reinforcements, in situ MMCs exhibit excellent mechanical properties.

MMCs are a kind of material in which rigid ceramic reinforcements are embedded in a ductile metal or alloy matrix. MMCs combine metallic properties (ductility and toughness) with ceramic characteristics (high strength and modulus), leading to greater strength to shear and compression and to higher service temperature capabilities. The attractive physical and mechanical properties that can be obtained with MMCs, such as high specific modulus, strength, and thermal stability, have been documented extensively. Interest in MMCs for use in the aerospace and

automotive industries and other structural applications has increased over the past 20 years. This increase results from the availability of relatively inexpensive reinforcements and the development of various processing routes that result in reproducible microstructure and properties.

The properties of MMCs are widely recognized to be controlled by the size and volume fraction of the reinforcements as well as by the nature of the matrix/reinforcement interfaces. An optimum set of mechanical properties can be obtained when fine, thermally stable ceramic particulates are dispersed uniformly in the metal matrix.

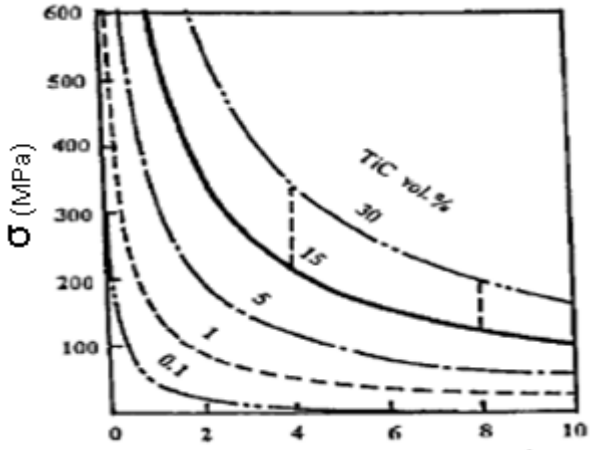

Figure 2.6 Increase in strength (r) of in-situ fabricated TiC-reinforced Al nanocomposites with increasing volume fractions or decreasing diameters of dispersed-phase (TiC) particles (Ajayan et al., 2003, p.16).

The homogeneity of composite materials is crucially important to high-performance engineering applications such as in the automotive and aircraft industries. A uniform reinforcement distribution in MMCs is essential to achieving effective load-bearing capacity of the reinforcement. Nonuniform distribution of reinforcement can lead to lower ductility, strength, and toughness of the composites. Nanoscale ceramic particles synthesized in situ are dispersed more uniformly in the matrices of MMCs, leading to significant improvements in the yield strength, stiffness, and resistance to creep and wear of the materials. The values of strength (r) increased with increasing volume fractions or decreasing diameters of dispersed-

phase (TiC) particles. When the volume fraction of dispersed particles is about 15–30 vol % and the particle diameters 40–80 nm, the values of r are 120–270 MPa and 200–350 MPa, respectively (see Figure 2.6 for details).

2.3.3 Thin-Film Nanocomposites: Multilayer and Granular Films

Thin-film nanocomposites are films consisting of more than one phase, in which the dimensions of at least one of the phases is in the nanometer range. These nanocomposite films can be categorized as multilayer films, where the phases are separated along the thickness of the film, or granular films, in which the different phases are distributed within each plane of the film (Figure 2.7). Multilayered thin-film nanocomposites consist of alternating layers of different phases and have a characteristic thickness on the order of nanometers. These films are usually used for their enhanced hardness, elastic moduli, and wear friction properties. The elastic modulus is higher in multilayered thin films than in homogeneous thin films of either component. The supermodulus effect is observed in some metallic systems, by which, at certain characteristic thicknesses (typically 2 nm, corresponding to a bilayer consisting of one layer of each phase) of the film, the elastic modulus increases by more than 200%. The most satisfactory explanation of this effect assumes an incoherent interface between the adjacent layers, suggesting that atoms are displaced from their equilibrium positions and that, during loading, all the layers undergo compression, which results in a higher resistance to deformation. The increase in hardness of the multilayer nanocomposites has been explained by considering that, when ultrathin films of materials with different dislocation line lengths are stacked, the strength approaches the theoretical limit. The dislocations cannot move from layer to layer, due to the difference in dislocation line lengths, and the films are thin enough that independent dislocation sources do not become operative. Conventional thin-film deposition techniques (sputtering, physical vapor deposition, CVD, electrochemical deposition, etc.) can produce multilayer nanocomposites, and the excellent flexibility of these techniques creates extremely thin films of uniform compositions.

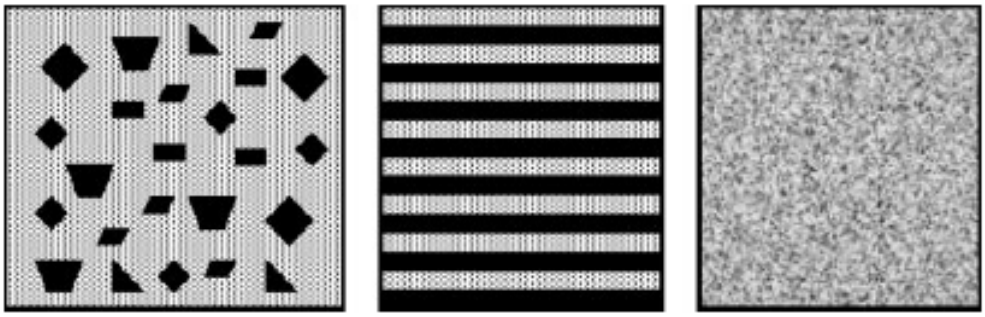

Figure 2.7 Schematic of possible microstructures for nanocomposite and nanostructured coatings: isotropic dispersed multiphase microstructure (e.g., TiC/amorphous carbon), multilayered microstructure (e.g., TiN/TiC) for nanocomposite coatings, and homogeneous alloyed microstructure as possible homogeneous nanostructured coatings (e.g., NiCoCrAlY alloy) (Ajayan et al., 2003, p.23).

2.3.4 Nanocomposites for Hard Coatings

Improved wear resistance, good high-temperature stability, and improved friction properties are important characteristics of good coatings for use in applications such as cutting tools. Most widely used coatings are made from TiN, TiC, TiAlN, CrN, diamond-like carbon (DLC), WC/C, MoS_2, Al_2O_3, etc. For improved coatings in which lower friction, increased life time, increased toughness, higher thermal stability, and in some cases, environmental (biomedical, for example) compatibility are needed, new types of materials are being considered, including nanocomposite materials. Nanocomposite structures such as multilayers or even isotropic coatings can be made from nanoscale entities with properties superior to single-phase materials. This approach of using nanocomposites is an alternative to using specific alloying elements in single-phase coating materials (to improve properties such as hardness) and provides far better flexibility in tailoring multifunctional coatings.

Nanocomposite coatings usually consist of two or more phases combined as multiple layers or as homogeneous isotropic multiphase mixtures. Classical multilayer (3 to many layers) coatings have total thicknesses of several micrometers, and the many layers are typically used to provide toughness (by crack deflection at the many interfaces) and properties such as oxidation resistance (due to, e.g., TiAlN layers). Building multilayer structures also provides better tribological properties. Gradient layers are also often introduced to counterbalance the vast differences in thermal expansion coefficients between multiple layers, which would cause internal

stresses and delamination at the interfaces between layers. In nanoscale multilayer coatings, when the thickness of each layer is in the nanometer range, superlattice effects can increase the hardness and other properties of the coatings. The increased hardness of such coatings (e.g., TiN/VN), where the superlattice period is a few nanometers, can be orders of magnitude higher than that of the corresponding base materials. The hardness increase in these nanoscale multilayer films results mainly from hindering dislocation movements across the sharp interfaces between two materials having vastly different elastic (particularly shear modulus) properties and lattice mismatch (coherency strain). One interesting point to note is that, if the individual layers are very thin (less than 3–5 nm typically), the hardness increase can disappear, because the strain field around the dislocations falls mainly outside the particular layer. Also, the sharpness of the interface also affects the hardening mechanisms, because high-temperature interdiffusion between layers can decrease the sharp variation in shear modulus. Another possible reason for increased hardness and improved chemical stability is chemical differences intentionally inserted at the interfaces so as to induce strains and electronic interactions; for example, TiAlN/CrN multilayer structures are more efficient than TiAlN films. The hardness effect resulting from lattice mismatch disappears at multilayer periods greater than 10 nm, due to lattice relaxation. Hence, for practical applications, the thickness of the layers in these coatings is designed based on the above considerations so as to obtain the optimum hardness values and wear properties with appropriate temperature stability. In fact, for many coating applications (e.g., coatings for cutting tools), toughness at high operating temperatures and chemical stability are more crucial than hardness alone. Commercial multilayer coatings with multilayer periods in the nanoscale range do exist; for example, WC/Co coatings used in the cutting tool industry. When the multilayer nanoscale coatings are deposited by periodic variation of the deposition (e.g., sputtering) conditions, a templating effect is often observed. In building superlattice structures from different materials of different structures, the layer first deposited can force the next layer (of the different material) to adopt the crystallographic structure of the first layer; this occurs, for example, in TiN/Cr_2N coatings in which Cr_2N is forced into the structure of the TiN (fcc) underlayer and in TiN/AlN, in which the AlN (originally wurtzite) is forced into the NaCl structure of the TiN (Ajayan et al., 2003, chap.1.6).

In addition to nanoscale multilayer coatings, it is also possible to fabricate isotropic nanocomposite coatings consisting of crystallites embedded in an amorphous matrix, with grain sizes in the nanometer range. These coatings generally have one phase that is hard (load bearing; e.g., transition metal carbides and nitrides) and a second phase that acts as a binder and provides structural flexibility (amorphous silicon nitride, amorphous carbon). The formation of these composite structures involves phase separation between two materials (which show complete immiscibility in solid solution), which are often codeposited, for example, by sputtering or plasma deposition. Unlike in multilayer composite systems, the possible material compositions and particle sizes in nanocomposite coatings are restricted by material properties and deposition conditions. Typically, these nanocomposite coatings are deposited by plasma-assisted chemical vapor deposition (PACVD) or physical vapor deposition (PVD). Very hard (50– 60 GPa) coatings of nanocomposites have been made from a TiN/α-Si_3N_4 system, using PACVD from $TiCl_4$, $SiCl_4/SiH_4$, and H_2 at about 600°C. The nanocomposite contains nanocrystalline TiN (4–7 nm) in a matrix of amorphous Si_3N_4. The gas phase nucleation (uncontrollable rates), chlorinated precursors (unreacted species remain in the process, contaminating the films), and high processing temperatures are disadvantages in this process. PVD processing can be used to prepare the same coatings by sputtering Ti and Si targets in nitrogen gas at room temperatures. The disadvantage is that the films are of inferior quality, and the hardness is lower than the PACVD-deposited nanocomposite coatings. In addition to improved hardness, nanocomposite coatings also show better oxidation resistance in comparison to TiN coatings.

It is interesting to note and analyze the high hardness of these nanocrystalline particles/ amorphous matrix coatings. Typically in single-phase nanocrystalline materials, the major increase in hardness comes from the lack of plastic deformation because the dislocations face far more barriers to mobility. However, hindered dislocation alone cannot explain the superior hardness properties of these nanocomposite coatings.

Other systems that create excellent nanocomposite-based, low friction, hard coatings are based on carbide particles (Ti, Ta, Nb, etc.) in diamond like carbon (DLC) matrices. Several techniques, such as PVD, pulsed-laser deposition, and reactive magnetron sputtering, are used to deposit these coatings. These typically contain larger crystalline particles (10–50 nm) surrounded by thick amorphous carbon coatings (5 nm). The particle sizes are large enough to allow dislocations but are too small for crack propagation. The larger grain separation allows incoherency strains to develop and, under loading, cracks to originate between crystallites, which allow pseudoplastic deformation. Thus, their hardness is also much higher (30 GPa) than that of single-crystalline carbide materials, and these coatings have, in addition, much higher toughness. These types of coatings can also be modified by introducing other elements; for example, W or Cr for creating optically absorptive coatings for solar energy converters and materials such as MoS_2 (TiN/MoS_2, TiB_2/MoS_2) for lubricating coatings.

Metal carbide/ductile metal systems are considered for cutting tools, because the carbide phase provides hardness and the metal provides toughness. For example, composites such as WC/Co, WC/TiC/Co are commonly used in cutting and forming tool applications, and these can be synthesized by various routes. These nanocomposites, in which the particle or grain sizes of the component phases are in the nanometer range, have much better mechanical properties (strength, hardness, toughness). Typically, reductive decomposition of W- and Co-containing salts, followed by gas-phase carburization (with CO/CO_2) are used to prepare nanocomposites such as WC/Co. These processes produce carbon-deficient metastable carbide phases with inferior mechanical properties. Alternative approaches, in which a polymer precursor such as polyacrylonitrile is used as the carbon source during the chemical synthesis and subsequent heat treatment to obtain high-quality nanocomposites (particle sizes 50–80 nm), have been developed. TaC/Ni nanocomposites are interesting from two aspects: excellent thermal stability and outstanding mechanical properties. They are used as surface coatings for protection against wear and corrosion. These nanocomposites can be prepared by devitrification of sputtered amorphous films of Na/Ta/C of nonstoichiometric composition. The grain size of the matrix Ni is about 10–30 nm, and the TaC

particles (10–15 nm) are uniformly distributed in the matrix. Even at 700^{o}C, no grain growth is observed, suggesting excellent thermal stability for these nanocrystalline duplex-phase composites. The measured hardness of the composite (12 GPa) matches that of conventional WC/Co nanocomposites at a much reduced volume fraction (35%) of the composite (Ajayan et al., 2003, chap.1.6).

CHAPTER THREE
ELECTRODEPOSITION TECHNIQUE

3.1 General Descriptions

The recognition that one might protect a surface from environmental attack, by application of an organic, inorganic or metallic coating, so extending the life of not just the surface, but the entire component or equipment, was one of the major advances in the history of technology. The implications, in allowing the use of less material or a less expensive material, coupled with the associated energy savings, have the profoundest economic consequences and underline the huge economic significance of surface engineering. Surface change as a result of external influences is given in Table 3.1.

Table 3.1 Surface change as a result of external influences (Kanani, 2004, p.2).

Surfece in contact with:	**Result surface change due to:**
Atmospheric air	Soiling, weathering
Hot gases	Oxidation, scaling
Flowing liquids	Cavitation, erosion
Micro-organisms	Microbiological damage
Chemicals	Chemical or electrochemical corrosion
Mechanical contact	Tribological damage, wear

Table 3.2 Coating processes used to protect functional surfaces (Kanani, 2004, p.3).

Process	**Process variants**
Evaporation	Chemical vapour deposition (CVD)
	Physical vapour deposition (PVD)
	Sputtering
Hot metal processes	Weld-surfacing
	Hot-dip galvanising
	Roll-coating
Painting	Application of inorganic coatings
	Application of organic coatings
	Application of low-friction coatings
Thermal spraying	Atmospheric-pressure plasma spraying
	Low-pressure plasma spraying
	Flame spraying
Metallising	Electroless metal coatings
	Electroplated metal coatings

The coating processes shown in Table 3.2 serve to illustrate the diversity of available and economically important processes which are commercially available

and can be used to protect surface functionality and towards extend the life of the component or equipment.

Whatever coating technique is used, it is almost invariably necessary to use the appropriate pretreatment and cleaning of the surface to maximise the performance of the coating. The processes shown in Table 3.2 will be briefly described below with comments highlighting major differences between them. There are lots of coating techniques such as; *Vacuum Evaporation, Weld-Surfacing; Molten Metal Coating Processes, Organic Coating, Painting, Thermal Spraying* and so on.

In addition to the coating processes detailed above, the *metallising of surfaces* has special importance. Here a metallic protective layer is applied to a surface as a coating for the component. Usually, this is carried out in aqueous medium. The metallic salt of the metal to be deposited, dissolved in solution, ionises and the metal cation is then discharged to form the metal itself, using an external voltage source. In other cases, a reduction medium is present in the electrolyte.

These processes are described as ***electrochemical or electroless surface metallising***, respectively. The latter process is widely used for metallising non-conducting materials such as plastics. The electrochemical method, also known as electroplating, is used for deposition onto metallic or other electrically conducting substrates, or to build up greater thicknesses on layers previously formed by electroless deposition.

The range of materials which, after the appropriate pretreatment and cleaning, can be coated in this way is extensive. In addition to plastics, it includes low-carbon and high-alloy steels, aluminium, magnesium and nickel alloys as well as cobalt and titanium based materials. In special cases, ceramic materials can also be metallised in this way.

3.2 Electroplating Processes

The electroplating of components both large and small, the latter sometimes known as mass plating is carried out using special equipment. Depending on the size and geometry of the components to be plated and the plating processes to be used, a distinction is made between rack plating, mass plating, continuous plating and in-line plating.

3.2.1 Rack Plating

Finished components or semi-manufactures, which, because of their size, shape or special features of construction, cannot be mass finished, are attached to racks, that is, fixtures suitable for immersion in the plating solution. Thus mounted, these are subjected to a suitable pretreatment and cleaning sequence, then plated and in some cases, subjected to a post-treatment. The process is sometimes known as batch-plating.

The attaching of components to the rack is usually done manually, often by means of copper wire. After this the racks are transferred, often by hand, to the first of the process tanks. After immersion for the prescribed time, the rack is withdrawn and moved on to the next bath, and so on until the sequence is completed. Finally, the plated components are thoroughly rinsed and dried and taken to the loading bay. Manual rack plating of this type (so-called manual plant) is by definition labour intensive and thus relatively expensive. However, it comes into its own when dealing with bent or tubular components. In such cases, the components mounted on the racks must be immersed in solution and agitated in such a way that electrolyte residues are completely drained. A degree of automation is found in the so-called semi-automatic plating plant. In this, the racks after they have been manually passed from tank to tank, in which they are mechanically agitated, are then automatically returned, after unloading, to the beginning of the cycle. In most cases, the racks are raised and lowered into the sequence of tanks using an overhead conveyor which is manually controlled. The main advantage of this approach is the reduction in the amount of manual labour involved.

A much-favoured system is the so-called fully automatic one in which the racks carrying the work are automatically transferred through the sequence of plating, post-treatment and rinsing tanks. The entire process is controlled either by a computer or a programmable logic controller (PLC) and not only the plating process itself, but the loading and unloading of the parts before and after plating are also controlled by the computer. In its most advanced form, bath analysis, dosing with additives, monitoring and control of bath temperatures and duration of bath immersion time are all automated (Kanani, 2004, chap.1.3.1).

3.2.2 Mass Plating

Among the various types of components which are plated, are small items such as screws or nuts. Rack-plating is not a feasible preposition in cases where throughputs may be millions of items per day. They are therefore processed by one or other methods known collectively as 'mass finishing'. Depending on their geometry, dimensions and shape, the plating of such items require special equipment. The most widely used system uses the so-called plating barrel. Also found are plating bells and vibratory plating units. Mass plating, though it offers many advantages, it is not suitable for delicate parts where there is a danger of deformation, scratching, or entanglement. Correct operation can minimise such dangers, and avoiding over-loading, under-loading, use of correct rotation speeds and adding 'ballast' to the work-load are among the means of ensuring optimum results (Kanani, 2004, chap.1.3.2).

3.2.2.1 Barrel Plating

Plating barrels, which have proved their worth in treatment of large quantities of small items by the mass finishing approach, are perforated barrels which are either cylindrical or polygonal in shape. Typically they rotate around either a horizontal or an inclined axis. For optimum performance, they are loaded with a single type of component, of a shape allowing the load to tumble readily during rotation of the barrel rather than rotating en masse as the barrel turns.

The barrel is usually loaded with small components which have been previously treated either mechanically or chemically in some previous operation. After loading, the barrel is sequentially transferred from pre-treatment tanks, through the various processing solutions and then on to post-treatment, after which it is withdrawn from solution. The entire sequence may be carried out semi-automatically with electric hoists, or it may be completely automated using a flight bars mounted on rails in much the same way as in various types of rack plating plant. The emptying of barrels and a drying of their plated contents can likewise be automated. The barrel rotation is powered in most cases by an electric motor which may have its own power supply or (less satisfactorily) it may draw power from the plating busbars. Barrels up to 2 m long and up to 1 m in diameter are used on larger plants. At the other extreme, they may be smaller than 5 cm in height and diameter (Kanani, 2004, chap.1.3.2.1).

3.2.2.2 Bell Plating

Plating bells are polygonal, bell-shaped containers which rotate around a vertical or near-vertical axis. They are perforated around their periphery and their floor and are specially suitable for the plating of smaller quantities of work. In consequence, they require smaller volumes of electrolyte. After loading with the work, the units are immersed in the electrolyte tanks and, after the prescribed length of time, withdrawn when plating is complete. In contrast to plating barrels, a useful feature of plating bells is that they allow random samples of the work to be withdrawn during operation without interrupting the plating process, for process monitoring and quality control (Kanani, 2004, chap.1.3.2.2).

3.2.2.3 Continuous Plating

The plating of metal strip, wire and tube is carried out in so-called continuous plating plants. In these, the items to be plated move continuously past either one row or between two rows of anodes at a substantial rate. It follows that operating conditions in such plants may be completely different from those found in the analogous batch plating operations. Provided the geometry of the work being plated

is simple and uniform, the process can deliver excellent results. Given the high deposition rate found in such plants, the necessary dwell time is a function of line speed and the length of the plating tank. For various reasons, it is sometimes necessary to configure such plants as a series of plating tanks through which the work passes, one after the other. Because of the high current densities used, electrolytes used in such continuous processes are characterised by their very high metal ion concentration and very high electrolytic conductivity. Since no great amount of throwing power is required, such electrolytes often contain no additives. Being very highly automated, such plants often require a minimum of supervision and maintenance.

A major advantage of continuous plating lines arises in the case of plated metal strip. In this case, coatings on either side of the metal strip need not be of the same thickness, resulting in great savings in the use of the raw materials and energy (Kanani, 2004, chap.1.3.2.3).

3.2.2.4 In-line Plating Processes

A development in recent years has been the integration of the plating and finishing processes into the main production line. This can bring many benefits including a significant reduction in use of eco-unfriendly materials. In-line plating also allows some pretreatment stages to be omitted, thanks to closer control of the plating and production lines and this again can reduce the consumption of chemicals.

The main benefits from using this approach, both economic and environmental can be summarised as follows:

- Savings in chemicals used,
- Reduced effluent discharge,
- Complete recycling of chemicals used in the process solutions and
- Reduced energy consumption (Kanani, 2004, chap.1.3.2.4).

3.3 Electroplating and Its Key Role

'Metal Finishing' is a term embracing the surface treatment and finishing of metals and nonmetals, in which a metallic coating is formed from an aqueous solution or a molten salt by means of an electrochemical reaction. The properties of such coatings are determined by the deposition process as well as pretreatment and post-treatments.

Metal finishing can be said to have transformed itself within a few decades from what was mainly an empirical craft, into a key technology, grounded on scientific principles. Coating methods have been systematically developed in terms of the composition and properties of the layer(s) required. Specific process parameters such as the deposition rate, deposition efficiency and throwing power of each electrolyte have been specially developed to meet the required specifications. In this way, one can now deposit either pure metal or alloy coatings of virtually any composition.

The properties of such metallic coatings are often different from those of the corresponding massive metal or alloy. The reason for this lies in the microscopic or sub-microscopic structure of such metal layers. Thus, the Vickers microhardness value is one of the simplest ways of demonstrating such differences. From the data in Table 3.3 it will be clear that electrodeposited metal coatings are uniformly harder than their counterparts prepared by metallurgical methods (Kanani, 2004, p.8).

Table 3.3 Vickers microhardness (HV) for selected metals (Kanani, 2004, p.9).

Metal	**Manufacturing process**	
	Metallurgical	**Electrodeposition**
Cadmium	30	50
Chromium	350	1000
Cobalt	200	500
Copper	50	150
Nikel	150	500
Zinc	30	130
Tin	10	10

Metal finishing as defined above, also includes the formation of conversion coatings. Composite coatings with a metal matrix and non-metallic inclusions (also

known as dispersion coatings) are finding growing application, while selective deposition is useful, for example, to repair defective or worn coatings, thus allowing recycling of components. Parts with complex shapes and surface topography can be manufactured by electroforming. Table 3.4 shows but a few of countless such examples.

Table 3.4 Protective layers and coating formed by metal finishing (Kanani, 2004, p.9).

Type of coating	**Example**
Metallic	Chromium, hard chromium precious metals (gold, platinum, palladium, rhodium, silver) copper, nickel, zinc, tin
Multi-layered	Copper + nickel; copper + nickel + chromium
Alloy coatings	Gold-copper-cadmium; copper-nickel-chromium; nickel-cadmium; nickel-cobalt; nickel-phosphorus; zinc-cobalt, zinc-iron; zinc-nickel; tin-lead: tin-cobalt
Composite coatings	Chromium + alumina; cobalt +chromium carbide; cobalt + chromium oxide; (nickel-phosphorus) +SiC; (nickel-phosphorus) + PTFE
Conversion coatings	Blacking, chromating, phosphating
Anodised coatings	Anodised aluminium, anodised magnesium: anodised titanium
Electroforming	Iron, copper, nickel, nickel-cobalt

3.4 Metallic Coatings

In the following, some of the examples shown in Table 3.4 and their typical applications are examined.

3.4.1 Chromium Coatings

Electroplated chromium coatings are notable for their high resistance to tarnish their high hardness and wear resistance as well as their low coefficient of friction resistance to cold welding. With a thickness of 0.2-0.6 microns and bright silver to matt appearance, they are widely used as decorative finishes. Thanks to this, special design effects can be achieved. While chromium deposits from hexavalent electrolytes are silver with a blueish tinge, those formed from trivalent chromium

baths can have an attractive smoky appearance. Black chromium deposits can also be formed, and a thickness from 0.5 to ~2.0 mm is often used for optical equipment and cameras. In contrast to decorative chromium, hard chromium deposits are usually much thicker, from 10 to 500 microns. They are typically applied to cylinder bores, valves and piston rods of diesel locomotive engines. As a result, service intervals between overhauls can be increased from around 10,000 km to over a million kilometers. Hard chromium plated components are widely used in the mining and aircraft industries and for hydraulics and metal deformation equipment. They are also used in the finishing of medical and surgical equipment (Kanani, 2004, chap.1.4.1.1).

3.4.2 Zinc Coatings

In the automotive industry, more than any other, the corrosion protection of functional components is considered to be vital. For this reason, such components are usually zinc-plated. Thereafter, such components are usually conversion coated, then sealed. In the past, chromate conversion coatings were the most widely used. Today, on account of environmental legislation restricting use of Cr(VI), alternative conversion coatings have been, and are being, developed. The corrosion resistance of conversion coated, zinc-plated components is so effective that the number of such components used in most vehicles, continues to increase. The pleasing colours of chromated finishes have in the past obviated the need for painting. However, as chromates cease to be used, this issue will have to be reconsidered. Thick-film Cr (III) passivates are blue in colour (Kanani, 2004, chap.1.4.1.4).

3.4.3 Composite Coatings

Composite coatings with an electrodeposited metal matrix and non-metallic inclusions have excellent wear resistance and permit emergency dry-running of machinery. Nickel coatings with 8-10 vol% of silicon carbide are used to increase the life of internal combustion engine cylinder bores, for example, in portable chain saws. Even though such coatings have also been used with aluminium cylinder blocks, they have been largely superseded by alternative coating methods. Composite coatings based on chromium carbide in a cobalt matrix are used as wear-resistant

coatings in gas turbines where they are required to perform for extended periods at temperatures of up to 800^{o}C Chromium deposits with alumina inclusions are used in piston rings for diesel engines. Single crystal diamonds locked into a nickel matrix form the cutting edge in tools such as chainsaws, grinding discs or dental drills (Kanani, 2004, chap.1.4.1.7).

3.5 Areas of Application

From the foregoing, the vital role of metal finishing in a wide range of applications can be appreciated, indeed in some cases, makes such applications feasible. Electroplated coatings must possess, according to their end use, various properties, either functional or decorative or both. Use of the correct coating can increase the life-time and service-interval of components or entire machines many times over. The parameters shown in Table 3.5, which include hardness, wear-resistance and coefficient of friction of either electroplated or electrolessly deposited coatings, are proof of this.

Table 3.5 Hardness, wear-resistance and coefficient of friction of electroplated or electroless coating (Kanani, 2004, p.13).

Coating	**Deposition rate (µm/min)**	**Hardness HV**	**Wear (mg x 10^{-3})[1]**	**Coefficient of friction**
Hard chromium	0.6-0.8	800–1100	0.9	0.15–0.18
Nickel[2]	1-10	200-450	4-5	0.4-0.6
Nickel (PTFE)	1-2	300	4-5	0.15-0.3
Nickel (SiC)	2-5	400-500	0.4-0.6	0.5-0.7
Nickel[3]	0.3	400-(700)	(2)-4	0.3-0.4
NiP (PTFE)	0.05-0.8	300-(700)	(0.7)-3	0.1-0.2
NiP (SiC)	<0.3	500-(>1000)	(0.2)-0.4	0.5-0.7
Ni Co-P (CF_x)	1-2	700-(1200)	2-3	0.1-0.15

Note: figure in parentheses are data after heat treatment.
[1]Data using Taber Abraser
[2]Electrodeposited
[3]Electroless deposition (the hardness values given in parentheses are achieved after heat treatment.).

Table 3.6 collates the most important properties of electrodeposited coatings and gives examples for their practical application in a range of industrial settings. The examples shown in Table 3.6 demonstrate how, by using electrodeposition processes to apply the correct type of coating, it is possible to enhance the properties of a substrate in specific ways. Thus, while the substrate material may provide adequate

mechanical properties, a coating can be necessary to provide sufficient corrosion protection, wear-resistance, hardness or tensile strength. This also highlights the difference between coatings with decorative and functional purposes, indeed coatings are often designated along these lines. Thus, functional coatings are applied to improve corrosion- and wear-resistance including dry-running or to improve solderability and weldability.

Table 3.6 Properties and applications examples of electrodeposited coatings (Kanani, 2004, p.14).

Coating property	**Application purpose**	**Example**
Optical Properties		
Colour	Aesthetic appearance	Brass-plated furniture and lighting fittings
Brightness	Decorative appearence/reflectivity	Chromium-plated taps, silver mirrors
Physical Properties		
Electrical conductivity	Current conduction on surface	Copper tracks on printed circuit boards
Thermal conductivity	Improved heat transfer on surface	Copper-plated saucepan bottoms for electric cookers
Magnetic conductivity	High coercivity	Cobalt-nickel alloys on magnetic storage
Chemical Properties		
Chemical protection	Resistance to corrosion attack	Lead-tin coatings as etched resistance for printed circuit boards
Corrosion protection	Resistance to corrosion attack	Zinc and its alloys on steel components
Mechanical Properties		
Ductility	Improved plastic performing	Copper coating on drilling punches in multi-layer printed circuit boards
Hardness	Improved adhesive wear-resistance	Nickel or phosphorus coatings for mining equipment
Technological Properties		
Friction reduction	Improved dry-running	Lead-tin-copper coatings
Adhesion	Improved adhesion	Brass coating on steel wires
Solderability	Soldering without aggressive fluxes	Zinc-lead coatings on printed circuit board tracks
Lubricity	Improved mobility	Copper plating for wire drawing
Wear resistance	Improved lifetime	Hard chromium-plated tools
Machinability	Metal machining	Copper coatings on printing cyliders

These coatings must also permit subsequent machining or manufacturing operations. In the case of decorative coatings, aesthetics are the primary concern, though adhesion of coating to substrate should not be overlooked. Increasingly, however, it is demanded that functional equipment should also be visually attractive,

and to make a sharp division between functional and decorative coatings could in many cases be misguided. The bottom line is to optimise functionality and appearance of component and coating, having regard to economic and environmental factors.

3.6 Processes for the Deposition of Metallic Coatings

A metallic coating can only be deposited onto a substrate from an aqueous solution of a metal salt if there are sufficient electrons available, from whatever source, to neutralise the metal ions in solution, allowing the metal itself to form in the zerovalent state. In practice, there are two main sources of such electrons, each forms the basis of a technologically important process.

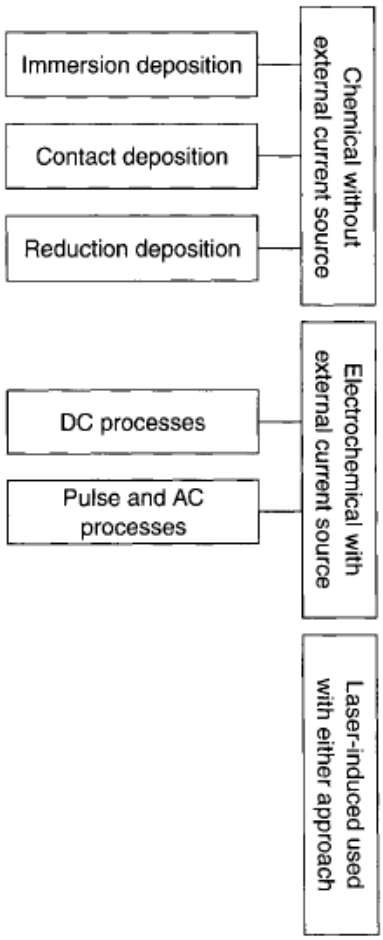

Figure 3.1 Chemical and electrochemical processes for deposition of metallic layers (Kanani, 2004, p.89).

The first of these is the so-called electroless or chemical deposition, which does not involve any external source of voltage or electron source. The second is the electrolytic deposition, where electrons are supplied from an externally applied voltage. Figure 3.1 provides an overview of both types and a variant, which is laser-induced deposition. The latter is a relatively new concept, reflecting the development of laser technology. It can be applied to either of the two main types of deposition. In the following treatment, these processes will be more closely examined.

3.6.1 Electroless Metal Deposition

The hallmark of this type of process is the absence of any external power source. Although they operate on very different bases, one should include three different types of process under this heading. Immersion plating, contact plating and chemical reduction plating. The first two are used only in very special situations. The last of the three is easily the most important and indeed 'electroless deposition' is widely used as a synonym for chemical reduction plating.

The operating principle of chemical deposition is depicted in Figure 3.2. The discharge of metal ions present in solution is achieved using a chemical reductant, R^{H+} in solution. This is not added to the solution, but is already present at the point the work is immersed in the electrolyte.

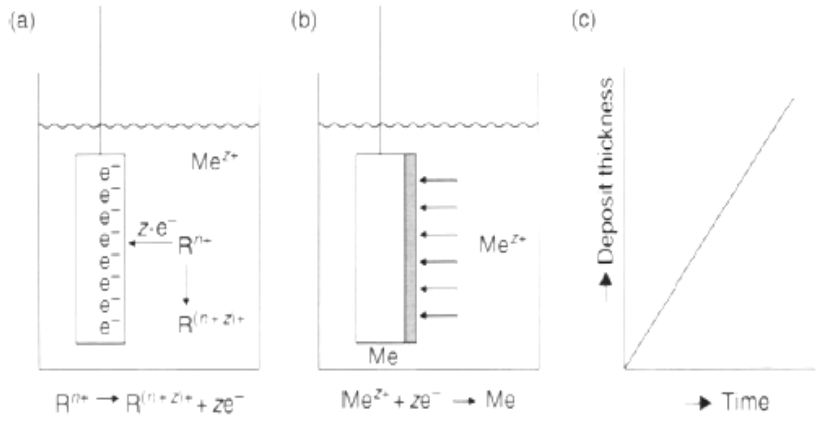

Figure 3.2 Principle of electroless deposition: (a) oxidation of the reductant; (b) reduction of the metal ion, leading to formation of the metal layer; (c) plot showing rate of deposition (expressed as thickness) versus time (Kanani, 2004, p.89).

A major advantage of chemical (electroless) deposition is that it can be used to metallise non-conductive surfaces, such as plastics, glass or ceramics. This requires a suitable pretreatment, in order to 'activate' these surfaces. This consists of a sequence of steps in which the surface of the work is modified, allowing spontaneous deposition to take place.

The best-known and perhaps economically most significant example is the metallising of printed circuit boards, and in particular, the through-holes in order to provide a conductive path from one side of a board to the other, or through a multilayer stack. Printed circuit boards are usually made of glass fibre-reinforced epoxy resin. The activation involves a number of stages, perhaps the most important of which is application of a $SnC1_2/PdC1_2$ solution, prior to electroless copper plating. Palladium nuclei form on the electrically non-conducting hole walls and these act as growth centers for the subsequent electroless copper deposition.

a) Deposition of metal layers

The overall process taking place in electroless deposition can be formulated as a true chemical reaction, in which no electron transfer is explicitly shown. This conceals, however, the actual electrochemical nature of the process, which can be written for the reduction of a z-valent metal as follows:

$$R^{n+} \rightarrow R^{(n+z)+} + z.e^{-}$$

$$\frac{Me^{z+} + z.e^{-} \rightarrow Me}{Rn^{+} + Me^{z+} \rightarrow R^{(n+z)+} + Me} \qquad (3.1)$$

This is known as a coupled reaction, comprising two half-reactions, the one anodic, and the other cathodic. Because the electrons donated by the reductant have nowhere to go, other than being accepted by the metal ion, the rates of these two half-reactions (in the absence of any complicating factors), have to be equal, and indeed to proceed at the rate of the slower of the two. In practice, the hydrogen evolution reaction offers a secondary, additional, cathodic reaction.

The net outcome of the coupled reactions, as seen in Eq. (3.1), is the deposition of the metal. Clearly it is desirable that the metal deposit on the surface of the work to be plated. However, this is not always the case. Thus, the metal can deposit in finely divided form in the electrolyte itself, and can also deposit on the walls of the electrolyte containing tank. Ensuring that the surface of the work to be plated is the preferable deposition site, must be a key aim. Although the substrate does not appear to be formally involved in Eq. (3.1), it functions as a catalyst for the point cease, unless the growing deposit itself were able to act as catalyst. Fortunately, in most cases, it does so, and thus as long as sufficient reductant and metal salt remain in solution, there is no limit to the thickness of an electroless deposit. For this reason, the process is often described as being'autocatalytic'. In this behaviour, 'electroless deposition' processes differ from 'displacement plating' (Figure 3.3). In this process, also known as cementation or immersion plating, a steel nail (for example) is immersed in copper sulfate solution. The less noble iron atoms dissolve, and an electron exchange takes place with the iron atoms ionising, and an equal number of copper ions being reduced to the metallic state. However, once the steel has become obscured by being covered with a thin layer of copper (usually less than 1 micron thick), the driving force for the reaction is removed and further reaction ceases.

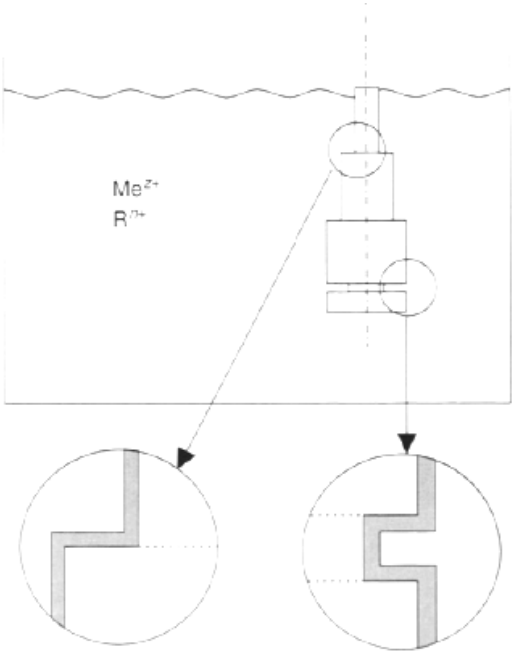

Figure 3.3 Electroless deposition makes possible uniform thickness coatings, even over the most complex geometries (Kanani, 2004, p.93).

These two processes, the one driven by a chemical reductant in solution, the other by a simple exchange of metal atoms at a surface, should not be confused.

b) Deposition of composite coatings

Deposits consisting of a metal matrix, in which particles of a second phase are distributed, either uniformly or with a concentration dependant on depth from the surface, are known as composite coatings or as dispersion coatings. They can be formed either by electrodeposition or, as discussed here, by electroless deposition.

The finely divided second phase particles which may range in size from 10 micron down to the nanometre range are may be inorganic or organic. Occasionally, they are metallic. Incorporation of such particles can greatly improve the mechanical properties of the deposit, notably friction and wear behaviour. Depending on the intended function of the coating, the second phase particles can be ceramics such as borides, carbides or oxides, they may be sulfides or PTFE (solid lubricants and low-friction), diamond or metallic, notably chromium which, after heat-treatment, yields alloys of the MCrA1Y family. Table 3.7 shows some of these, as used with an Ni-P matrix (Kanani, 2004, chap.4.2.3).

Table 3.7 Commonly used second-phase particles in electroless nickel matrix composite coatings (Kanani, 2004, p.93).

Carbides	**Oxides**	**Miscellaneous**
Cr_3Cr_2	Al_2O_3	c-BN
SiC	Cr_2O_3	CaF_2
TiC	SiO_2	Diamond
	TiO_2	MoS_2
		PTFE

3.6.2 Electrolytic Metal Deposition

The fundamental principle of the electrodeposition of a metal is shown in Figure 3.4. From this, it is seen that when a metal is immersed in an electrolyte solution, under certain conditions, a spontaneous dissolution takes place whereby metal atoms leave the metal lattice to form positively charged ions (cations) which migrate into the electrolyte. As a result of this so-called anodic dissolution, an excess of positively

charged ions is found in the immediate vicinity of the metal electrode. Their departure leaves an equal and opposite negative charge on the metal. Electrostatic charge attraction has the opposite effect and seeks to pull the positively charged ions back to the negatively charged metal. These processes, which can be described as a dynamic equilibrium, can be represented as:

$$Me \leftrightarrow Me^{z+} + z.e^{-} \qquad (3.2)$$

The double arrow indicates that equilibrium is reached by virtue of the process going from left to right and vice versa at the same rate. The potential difference $\mathrm{Aq} \cong \frac{\mathrm{eMe}}{\mathrm{MeZ^{+}}}$ (sometimes known as the metal-solution potential difference) has a fixed value for a given metal, immersed in a solution of Standard composition, pH and temperature.

The foregoing treatment does not explain what drives the metal atoms out of the lattice, or how the necessary energy to do so is acquired. The main source of such energy lies in the free energy of hydration of the metal ions so formed.

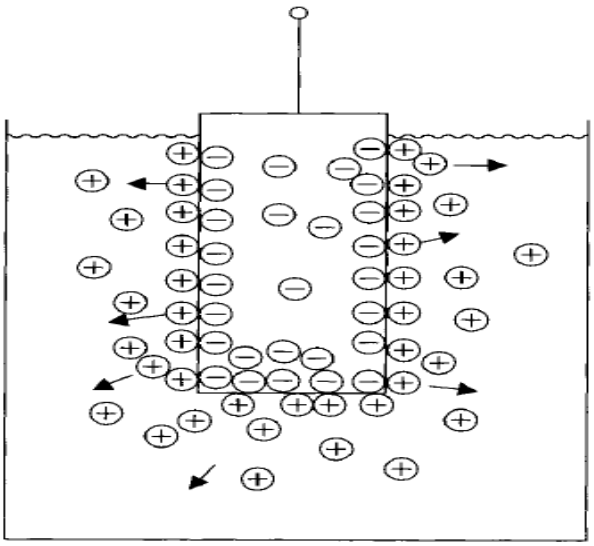

Figure 3.4 Spontaneous establishment of a charge at a metal-solution interface for a metal immersed in aqueous solution (Kanani, 2004, p.95).

The process of anodic dissolution or cathodic metal deposition implies movement of charge and thus constitutes an electric current, which is denoted as anodic or cathodic, respectively. Under a purely arbitrary convention, anodic current (I_a) is deemed to be positive, cathodic current (I_c), is negative. In some cases, *total* current is the relevant parameter. In other cases, current density, that is, current per unit surface area, is the critical parameter. Current density is sometimes denoted by i_a or i_c, and j is another symbol found in the literature for this. At equilibrium, the anodic and cathodic currents are equal, and no net current then flows. This can be represented as:

$$|I_c| = |I_a| = I^0 \quad \text{or} \quad |i_c| = |i_a| = i^0 \tag{3.3}$$

Here, i^o is the so-called exchange current density. In many sources, it is shown as i^o. It is an indication of the rate at which the dynamic equilibrium shown in Eq. (3.3) is taking place. Under equilibrium conditions, no net reaction takes place. However, if the metal is no longer at open circuit, but attached by means of a wire, for example, to an electron source or electron sink, this equilibrium will be disturbed. Attached to an electron source, more electrons will flow into the metal, which will become more negatively charged, and will attract more cations from solution. The metal is then said to be cathodic, and electrodeposition takes place. If the metal is connected to an electron sink, the metal will become positively charged, or 'anodic' and repulsion of metal cations will be encouraged, in other words, anodic metal dissolution.

The first of these is the basis of metal deposition or electroplating. Until quite recently, the process was carried out using direct current (DC). More recently, the benefits of using interrupted current or even cathodic current with periodic polarity reversal, have become clear and this is known as pulse current plating (Kanani, 2004, p.96).

3.6.2.1 Direct Current (DC) Electrodeposition

DC electrolysis can be represented as in Figure 3.5, where two electrodes, immersed in solution, are connected to the output of a DC current source. The cathode, onto which the metal (or alloy) is deposited, may itself be a metal or it might be a semiconductor or a non-metallic conductor such as graphite. Also shown in the Figure 3.5, is the anode. The primary purpose of this is to complete the electrical circuit, and as metal cations are removed from solution as the metal, so one or more balancing processes must take place at the anode to remove anions and thereby maintain overall charge neutrality in solution. The anode may or may not fulfil a second function, which is to provide a source of flesh metal to replace that which has been removed from solution by deposition at the cathode. Anodes fall into two classes. Sacrificial anodes are made of the same metal that is being deposited, e.g. copper. A copper anode will anodically dissolve, so releasing into solution copper ions to replace those which have been deposited at the cathode. Ideally the anodic process would be the absolute mirror-image of that taking place at the cathode. In practice, one or both processes are less than 100% efficient, and some sort of adjustment is required.

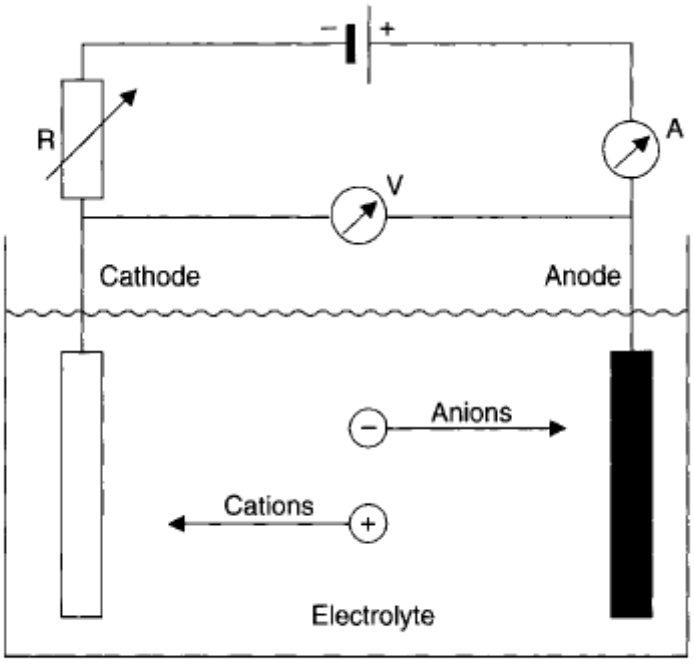

Figure 3.5 Main components of a DC electrolysis system (Kanani, 2004, p.97).

The second type of anode is the so-called permanent anode, typically platinum coated titanium. Where these are used, metal ion depletion from solution is made good by adding metal to solution in the form of a metal salt, for example, copper sulfate (Kanani, 2004, p.96).

a) Deposition of metal layers

If a voltage is applied across the two electrodes in an electrolysis cell, a current consisting of electron flow, will be set up, with these moving from the anode, through the external circuit and back to the cathode. The anode will thereby dissolve anodically, and the cations so formed will migrate to the cathode. Anions present in solution will move in the opposite direction towards the anode. Current will thus flow through the solution by virtue of the movement of these charged ions and this is known as ionic current, or electrolytic conductance.

Of critical importance in electrodeposition, is the mechanism by which metal cations are delivered to the cathode and the means for their replenishment as they are lost to solution by deposition at the cathode. The rate, at which flesh ions (and also uncharged species required for reaction) are delivered to the cathode surface from the bulk of solution, depends on the prevailing hydrodynamic conditions at and near the cathode surface.

There are three main mechanisms involved in delivery of ions to the electrode surface, these being migration (under a potential gradient), diffusion (under a concentration gradient) and convection (movement of the electrolyte liquid itself) (Kanani, 2004, p.98).

b) Deposition of composite layers

The properties of electrodeposited metals or alloys can be substantially modified, usually for the better, by arranging that finely divided particles are co-deposited with the metal or alloy, thereby becoming incorporated into a metallic matrix.

This is usually accomplished either by arranging for the particles to remain suspended in solution, or for them to settle onto a horizontal cathode surface over which the metal electrodeposits. Such particles may be inorganic (oxides, carbides, diamond), metallic (chromium) or organic (PTFE). The amount of second-phase particles thereby incorporated will be a function of the deposition conditions (pH, temperature, viscosity, concentration of particles in suspension, hydrodynamic conditions) and to the extent these parameters affect the zeta potential, this too is important. The particle size will be from 30 microns downwards, more recently there has been emphasis on nanometer-sized particles of 100 nm or less. The incorporation of such particles affects both the structure of the metallic deposit and its properties. Thus internal tensile stress can be reduced and thus the propensity to crack (particles can act as crack-stoppers). Surface properties such as friction and wear will likewise be modified and bonding characteristics also.

The choice of second-phase particle for incorporation depends on the function it is desired to enhance. For increased hardness, tensile strength and high-temperature characteristics, hard compounds such as the carbides of chromium, silicon, titanium or tungsten can be used, as can the oxides of titanium, silicon, aluminium and zirconium. Titanium nitride has also been used. Where tribological factors are important, boron nitride, graphite, fluorinated graphite, molybdenum disulfide and PTFE are used.

The action of such solid lubricants is usually initiated after a thin outer skin of pure metal has been worn away, after which their respective actions begin to operate. Many other species have also been used as second phase. Among these, three will be mentioned, namely diamond (for obvious reasons), metallic chromium particles which, after heat-treatment, alloy with the matrix to form an alloy which could not have been formed by simple electrodeposition of ions. Lastly, a technology has been developed for incorporation of micro-capsules which can be filled with whatever species is desired, liquid or solid, this being released as the surface wears away to expose fresh capsules. One particular application of composite coatings is the provision of surfaces which can, under emergency conditions, continue to function in the dry-running, that is, in the unlubricated state.

Table 3.8 Overview of electrodeposited coatings (Kanani, 2004, p.109).

Matrix metal	**Oxides**	**Carbides**	**Sulfides**	**Sulfates**	**Others**
Ag	Al_2O_3	SiC			
Au	Al_2O_3	SiC			
Cd	Fe oxide	SiC, WC			
Co	Various oxide				Natural or synthetic mica
Cr	Al_2O_3				
Cu	Al_2O_3, CeO_2, TiO_2, ZrO_2	SiC, WC, ZrC	MoS_2	$BaSO_4$, $SrSO_4$	Mica graphite
Fe	Al_2O_3, Fe oxide	SiC, WC	MoS_2		Natural or synthetic mica
Mn		SiC			
Ni	Al_2O_3, BeO_2, CdO, CeO_2, Fe oxide, MgO, SiO_2, ThO_2, TiO_2, ZrO_2	SiC, VC, WC	MoS_2	$BaSO_4$	Boron nitride, Teflon (PTFE), mica

The properties of composite coatings depend also on the particle size and distribution of the second phase. The growing use of sub-micro metre particle sizes (100 nm or less) has been mentioned and in certain applications, the second-phase must be high-temperature resistant, that is it must neither break down nor alloy with the matrix metal. The presence of such particles can create a dispersion-hardening effect in that they hinder dislocation formation in the grain, and act as pinning agents. In the same way, they can also hinder grain growth resulting from annealing.

Table 3.9 Industrially important composite coating (in grey) in possible future developments (Kanani, 2004, p.109).

Composite coating	**Application areas**
Co-Cr_2O_3/Co-Ni-Cr_2O_3	High-temperature resistant coating, aerospace
Me+graphite, Me+oil	Wear-resistant coating including dry-running
Ni- Al_2O_3+Cr-layer	For decorative uses
Ni-BN, Ni-graphite, Ni-MoS_2	Automotive industry
Ni-PTFE	Low-friction coating, automotive industry
Ni-SiC	Wear-resistant coating, automotive industry
Ni+diamond	For microelectronic uses
Ni+$NiFeS_2$.Cu+Cu_2O.Ni+TiO_2	Catalytically active surfaces
Ni+Cr+Al+Si+TiO_2	Dense, temperature-resistant coatings
Zn+SiO_2	Corrosion-resistant coatings

Table 3.8 gives an overview of matrix-second phase combinations while Table 3.9 shows those which are of industrial importance (Kanani, 2004, chap.4.3.1.3).

Where it is desired to achieve a uniform distribution of second phase through the matrix (and in some cases, a graded rather than a uniform distribution is sought), the second phase particles must be uniformly suspended in the electrolyte. For this to be so, the tendency to settle under gravity must be constantly overturned, by means of stirring, pumped electrolyte flow, ultrasonic agitation or air injection.

Sacrificial anodes are made of the same metal that is being deposited, for example, copper. A copper anode will anodically dissolve, so releasing into solution copper ions to replace those which have been deposited at the cathode. Ideally, the anodicprocess would be the absolute mirror-image of that taking place at the cathode.

In practice, one or both processes are less than 100% efficient, and some sort of adjustment is required. The second type of anode is the so-called permanent anode, typically platinum coated titanium.

In the case of very fine particles, a suitable surfactant is frequently added which, after ionising in solution, adsorbs on the surface of the particles and then Orient themselves according to their electric charge. The repulsive electrostatic forces thereby minimise coagulation of the particles, which could result in settling.

A number of workers have investigated the mechanism of the electrodeposition of composites, and most of their proposed mechanisms involve one or more of the following three processes (Kanani, 2004, chap.4.3.1.3).

1. Electrophoretic movement of positively charged particles to the cathode,
2. Adsorption of the particles at the electrode surface by van der Waals forces, and
3. Mechanical inclusion of the particles into the layer.

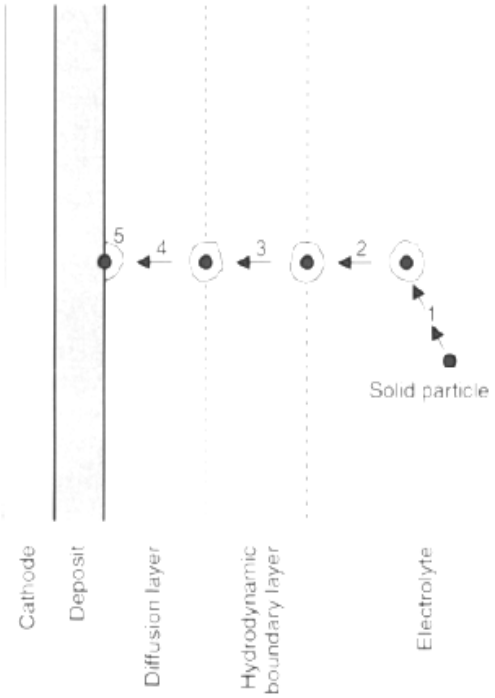

Figure 3.6 Process steps in codeposition and incorporation of a solid particle into the deposit; formation of an ion cloud around the particle (1); transport by means of convection (2); transport by diffusion (3); reduction reaction (4); adsorption (5) (Kanani, 2004, p.112).

These models are all, to a greater or lesser extent, approximate solutions, based on simplifying assumptions. As a result, they cannot be used for exact quantitative predictions. Even so, they are of value in pointing the way towards advances in the technology. They allow one to envisage the overall deposition process in terms of five discrete steps, shown in Figure 3.6.

These steps mark the progress of particles from the bulk solution to their incorporation in the deposit. The first stage postulates formation of an electro-active ionic cloud surrounding the particle, as soon as these are introduced into the electrolyte.

Under the action of convection, these ionically enveloped particles are transported to the hydrodynamic boundary layer, migrate across this and are conveyed by diffusion to the cathode. After the ionic cloud is wholly or partly reduced, the

particles are deposited and incorporated in the matrix as the metal ions are discharged, so 'burying' the inert particles.

3.6.2.2 Pulse Current (PC) Electrodeposition

Electrodeposition using pulsed currents, usually known as 'Pulse plating', is a relatively new approach. Though electrodeposition was traditionally carried out using DC, a modification of this by use of current interruption or even current reversal, goes back many years, as does the use of AC, superimposed on DC. Given that only electromechanical switchgear was then available, the timescale of these operations was many seconds in duration. Only with modern electronic switching has it become possible to create the short duration, but heavy current square-wave pulses shown in Figure 3.7. These pulses can be unipolar ('on-off') or bipolar (current reversal, with or without additional 'rests'). In all cases, the option remains to use pulses alone, or to superimpose these on a DC feed. Figure 3.7 shows the most common variants. In the case of the bipolar pulse, metal deposition occurs in the cathodic pulse with a limited amount of metal being re-dissolved in the anodic period. This repeated deposition and partial re-dissolution can improve the morphology and indeed the physical properties of the deposit.

In Figure 3.7, the area enclosed by the square waves represents electrical charge (i x t). Areas designated as 'k' represent metal deposition charge. Those with 'a', the re-dissolution. Clearly k must be greater than a, or no net deposition would take place. Also to be seen in Figure 3.7 are the rest periods between pulses, when no current flows.

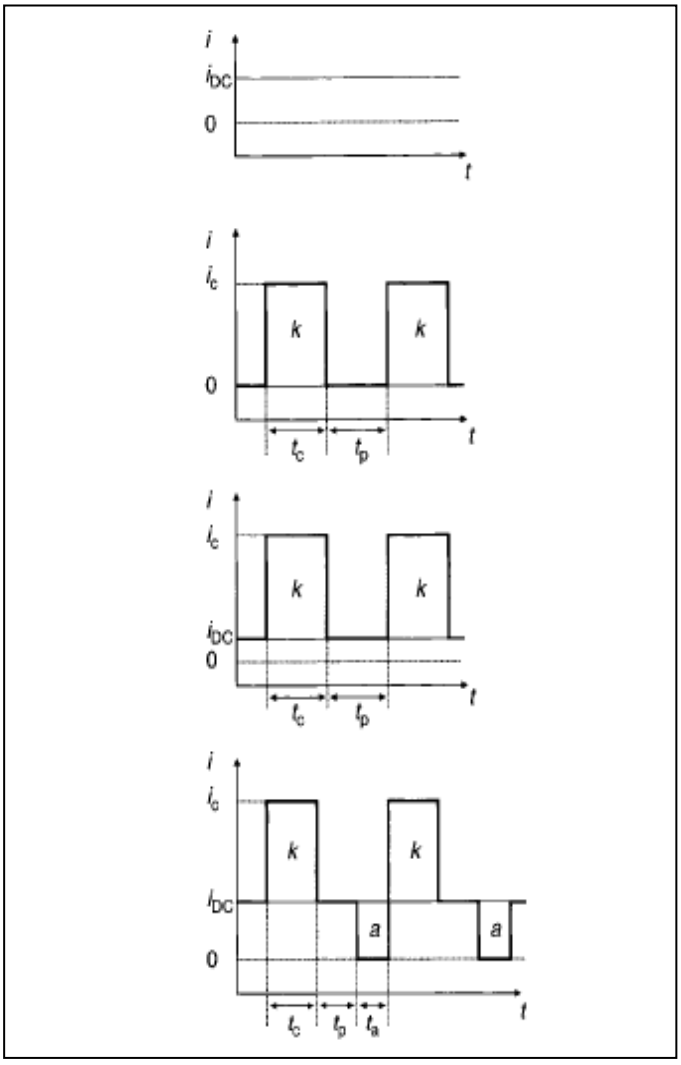

Figure 3.7 Typical current-time sequences (pulse) used in metal deposition by pulse plating. Top to bottom: single square-wave; square-wave superimposed on DC; square-wave superimposed on DC with polarity reversal. (uppermost: conventional DC electroplating current) (Kanani, 2004, p.119).

For some deposition processes, even more complex pulse trains than those shown in Figure 3.7 have been used. The function of the rest periods and reverse pulses is complex, and partly based on empiricism. However, it is clear that during the rest period, the concentration of metal ions in the Nernst layer can be replenished, so that when the cathodic polarity is again switched on, the deposition process takes place with a higher concentration of metal ions than would be found using all but the lowest DC current densities. It will also be noted that, as a consequence of pulsing,

the electrical double layer, which is analogous to an electrolytic capacitor, is repeated charged up and discharged. It should also be pointed out that, although the cathodic current might be applied for less than half the total time (Figure 3.7), the overall metal deposition rate can be as great or even greater than that obtained with DC alone (Kanani, 2004, p.117).

One implication of pulse plating is that, in addition to the usual independent variables in electrodeposition (pH, temperature, current density, bath composition, and agitation) one now acquires further degrees of freedom in terms of pulse duration, polarity, pulse height, etc. Expressing these as i_c (cathodic pulse height), tc (duration), t_{off} (off-time), i_a (anodic pulse height), tc and i_{DC} (DC current over which pulses are imposed), it is seen that at least five additional variable are now added to the list.

These parameters can be used to calculate current densities at each point in the sequence, though it has to be said, with the process now being describable as 'nonsteady- state', the concept of current density has little practical significance and it may be more meaningful to think in terms of total cathodic and total anodic charge passed over time, or their algebraic sum.

3.6.2.2.1 Pulse Current. In pulse electrodeposition (PED) the potential or current is alternated swiftly between two different values. This results in a series of pulses of equal amplitude, duration and polarity, separated by zero current. Each pulse consists of an ON-time (T_{ON}) during which potential and/current is applied, and an OFF-time (T_{OFF}) during which zero current is applied as shown in Figure 3.8.

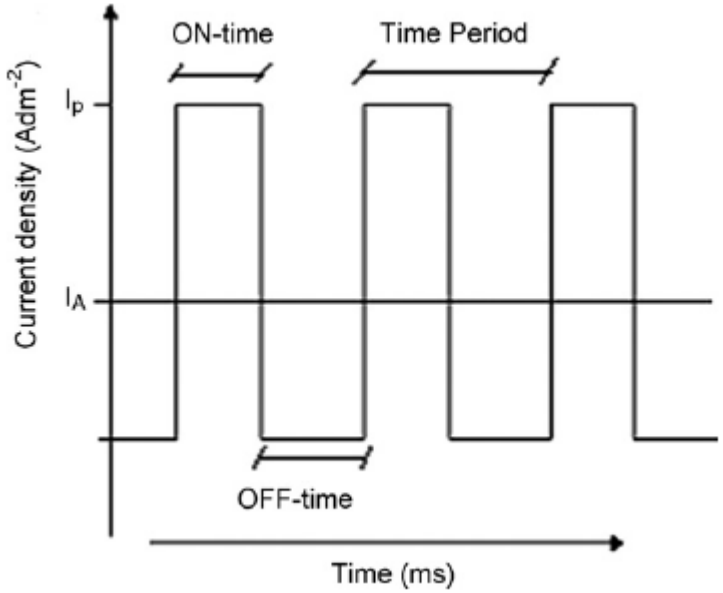

Figure 3.8 Typical pulse-current waveform (Chandrasekar et al. 2008).

It is possible to control the deposited film composition and thickness in an atomic order by regulating the pulse amplitude and width. They favor the initiation of grain nuclei and greatly increase the number of grains per unit area resulting in finer grained deposit with better properties than conventionally plated coatings. Process and circuitry for generating current pulses for electrolytic metal deposition are dealt in literature.

3.6.2.2.2 Types of Pulse Waveform. Modern electronics and microprocessor offers the flexibility of programming, of the applied current waveform. The latter is of two groups: (1) unipolar, where all the pulses are in one direction (with no polarity) and (2) bipolar, where anodic and cathodic pulses are mixed. There are many variants on these, but the number of variables increases with complexity of the waveform, which makes it more difficult to understand how a particular waveform affects the deposition. Typical waveforms include:

(1) cathodic pulse followed by a period without current (or an anodic pulse),
(2) direct current (DC) with superimposed modulations,
(3) duplex pulse,
(4) pulse-on-pulse,

(5) cathodic pulses followed by anodic pulses-pulse reverse current (PRC),
(6) superimposing periodic reverse on high frequency pulse,
(7) modified sine-wave pulses and
(8) square-wave pulses.

Among these, the *square wave pulses* have the advantage of an extensive duty cycle range (Chandrasekar et al. 2008).

3.6.2.2.3 Concepts of Pulse and Pulse Reverse Techniques. In electroplating, a negatively charged layer is formed around the cathode as the process continues. When using DC, this layer charges to a defined thickness and obstructs the ions from reaching the part. In PED, the output is periodically turned off to cause this layer to discharge somewhat. This allows easier passage of the ions through the layer and onto the part. (b) High current density areas in the bath become more depleted of ions than low current density areas. During T_{OFF}, ions migrate to the depleted areas in the bath. When pulse T_{ON} occurs, more evenly distributed ions are available for deposition onto the part. The effects of PC & PRC variables on electrodeposition are summarized in literature.

Permaloy Corporation has studied pulses superimposition on DC. Duplex pulse systems feature a burst of pulses at one level followed by a burst at another, all in one direction. Pulse-on-pulse systems offer complex wave shapes that have pulses at amplitude riding on top of those of lower amplitude. In PRC technique (Figure 3.9), plating current is interrupted and a stripping time is introduced into the plating cycle. PRC have the same effect of replenishing the diffusion layer like PC and selectively dissolves the protrusions of the metal surface to ensure a uniform deposit. The introduction of high frequency PRC reduces the use of additives, which limits the deposit ductility and electrical conductivity. PRC avoids the drawbacks of additives while the superimposed pulsation keeps control of the crystal structure (Chandrasekar et al. 2008).

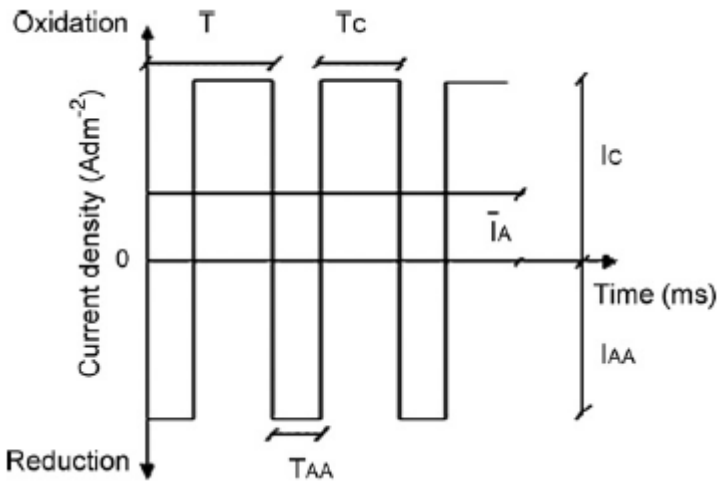

Figure 3.9 A typical pulse reverse waveform where, TAA is the anodic time, TC is the cathodic time, IAA is the anodic current density, IC is the cathodic current density, IA is the average current density, T is the cycle time.

3.6.2.2.4 Pulse and Pulse Reverse Current Parameters. In the conventional DC plating there is only one parameter, namely current density (I), which can be varied. But in PED we have three independent variables, viz, (i) ON-time (T_{ON}), (ii) OFF-time (T_{OFF}) and (iii) peak current density (I_P).

In PC, the duty cycle (γ) corresponds to the percentage of total time of a cycle and is given by:

$$duty\ cycle = \frac{T_{ON}}{T_{ON} + T_{OFF}} = T_{ON} f \qquad (3.4)$$

where *f* is frequency, defined as the reciprocal of the cycle time (*T*).

$$Frequency = \frac{1}{T_{ON} + T_{OFF}} = \frac{1}{T} \qquad (3.5)$$

In practice, pulse plating usually involves a duty cycle of 5% or greater and T_{ON} from s to ms. PC will deposit metal at the same rate as DC provided the average pulse current density equals the latter. The average current density (I_A), in pulse plating is defined as:

$$I_A = \text{peak current } (I_p) \times \text{duty cycle } (\gamma) \quad (3.6)$$

In case of PRC technique, the average current ($\bar{I}_A$) is as given below:

$$I_A = \frac{I_C T_C - I_{AA} T_{AA}}{T_{AA} + T_C} \quad (3.7)$$

In PRC, the duty cycle (γ') is given as below

$$\gamma' = \frac{T_C}{T_{AA} + T_C} \text{ with } T_{AA} = T_C \quad (3.8)$$

where I_C is the cathodic current density, I_{AA} is the anodic current density, T_{AA} is the anodic (reverse) time, and T_C is the cathodic (forward) time. The current efficiency of PRC is always less than that of PC (Chandrasekar et al. 2008).

3.6.2.2.5 Pulse Current and Duty Cycle/Frequency. For the same IA, the rate of metal deposition in PC could be same as DC plating. At low duty cycle, high IP is required to obtain the same average deposition rate as DC. With increasing duty cycle PC approaches DC and so duty cycle of 33–50% is taken as the minimum value.

At high frequency (*f*), the double layer does not have time to charge fully during the T_{ON} or fully discharge during the T_{OFF}. The PC diffusion layer consists of a stationary layer and a pulsating layer. The total diffusion layer thickness is equivalent to that obtained in DC plating thereby limiting the maximum frequency to ~500 Hz. However, at very high I_P, higher frequencies can be employed as charging and discharging of the double layer becomes shorter. The enhanced PC plating rates are mainly due to its effect on electrocrystallization (Chandrasekar et al. 2008).

3.6.2.2.6 Pulse Current and Current Distribution. Current distribution depends on potential distribution and the local concentration of electroactive species at the electrode surface. At increased current density, the throwing power deteriorates due to dominating primary current distribution. Higher I_P during T_{ON} results in less uniform current distribution irrespective of pulse waveform. PC may improve the

throwing power by altering the electrolyte's efficiency, hydrogen discharge and deposition mechanism.

3.6.2.2.7 PC and PRC Deposition of Individual Metals and Alloys

a) Deposition of metal layers (Chromium and its alloys)

The current efficiency of chromium deposition from the conventional sulfate baths were increased to 38% under low and high frequency PC plating when the anodic to cathodic charge ratio lies between 0.002 and 0.0085. The unipolar pulses and PRC technique reduces the stress enabling the production of crack-free deposits. PC plated chromium deposits were observed to have refined grains with enhanced hardness (close to 1000 HV), surface crack density and corrosion resistance than that plated with DC at same current density.

The HCP structured chromium deposits obtained at $60Adm^{-2}$ and pulsating frequencies between 0.05 and 1 kHz [66] were changed to BCC at higher frequencies (5–50 kHz) possessing superior mechanical property. The size of the nodules and the wear resistance depends on the chrome growth kinetics and T_{ON}/T_{OFF}. Multilayer Cr–Ni, with alternate amorphous chromium-rich layer and equiaxed grains of close to 7 nm in nickel-rich layer were produced using PC (Chandrasekar et al. 2008).

b) Deposition of composites layers

The deposition of metal matrix composites where the second phase is electrically conducting is more difficult than the co-deposition of non-conducting particles. The incorporation of second-phase particles in the growing metal matrix is usually governed by the adhesive forces at the particle-electrolyte interface, since these determine the transport of the particle through the diffusion layer, and its behavior there. In contrast to non-conducting particles, whose maximum incorporation rate, determined by the weak adhesion forces, is reached only when a given flow-rate is reached in solution, the behaviour of conducting particles is rather different. Incorporation of these species begins only when the deposition itself commences and is mass-transport determined.

The rate of incorporation remains virtually constant, once the layer is saturated with these species and, because of the strong adhesion forces in this case, is barely affected by hydrodynamic conditions in the electrolyte. Other significant parameters in the case of electrically conductive species include the stability of the particles in the electrolyte and their behaviour after incorporation in the growing deposit. Last but not least, the possible effect of such conductive particles on current distribution must be considered.

Thus, it appears that the behaviour of electrically conducting particles and the factors which influence them, are quite different from those acting in the case on nonconducting particles. It has been shown that modulation, for example, pulse plating, can be used in the deposition of metal matrix composites. Thus the deposition of nickel-cobalt matrix layers with zirconium inclusions over carbon-fibre reinforced carbon (CFRC) components was carried out in this way. CFRC, itself a composite, is based on carbon fibers in a carbon matrix.

This type of material is widely used for heat shields in space vehicles or as insulation in high-temperature furnaces. The high-temperature stability of CFRC can be further improved by coating it with a crack-free, non-porous composite coating which, by suppressing oxidation of the carbon, allows the material to function up to the limit of its thermal stability. Heat-resistant composite coatings include binary or ternary alloys of aluminum, chromium, iron, cobalt, nickel and silicon in various compositions, and suitable metal particles are incorporated into such alloys. Most such alloys cannot be simply electrodeposited from a solution. In the case of nickel and cobalt, this is straightforward since the reversible potentials of the two metals lie close to one another. The co-deposition of chromium is problematic, because of its very different reversible potential. However, the incorporation of zirconium particles in a nickel-cobalt matrix seems to be entirely feasible. The process is based on an electrolyte with a Ni:Co concentration ratio of 8:2 to 2:8. Zirconium particles of mean size 1-5 microns and at a suspension concentration of 50 g/1., A current pulse regime of 50:20 was found optimal. The Ni-Co matrix with Zr second phase deposit showed no significant internal stress. Nor were surface pores, pits or cracks due to

hydrogen bubbles a problem, since the hydrogen was able to diffuse away from the surface in the off-time. These deposits showed no dendritic growth at edges and surface rugiosities, such as might have been expected where electrical field lines were most concentrated. Presumably the zirconium particles behave as an electrically neutral species. The surface structure of this deposit did not display any non-uniformity at least up to a 3 mm thickness (Kanani, 2004, p.129).

PED improved the hardness (close to 500 $kg.cm^{-2}$) of Ni/SiC composite coatings at longer T_{OFF} that favored grain refinement of nickel and SiC incorporation. PRC technique improved SiC content in the composite by six times.

The tribological behavior of the Ni–P–SiC composite was beter than that of DC plated deposits. Microhardness of PC plated Ni–diamond composite (611 HV) is higher than that of DC plated composite (540 HV). The grain size and hardness of PRC plated Ni–Co/nanoalumina composites were better than those of DC plated composites due to enhanced nucleation rate. Due to partial dissolution of nickel in the anodic cycle, Ni–C nanofiber composite obtained by PRC technique had 5–6 wt.% higher fiber content (Chandrasekar et al. 2008).

3.6.2.2.8 Advantage of Pulse and Pulse Reverse Techniques.

(i) While PED significantly raises the limiting current density (I_L) by replenishing metal ions in the diffusion layer only during T_{OFF}, PRC does it continuously.

(ii) In PED, by modifying pulse parameters, deposits with desired composition, structure, porosity and hydrogen content could be obtained.

(iii) Pulse plating reduces the additive requirement by 50–60%. PRC enhances the bath stability and efficiency with negligible additive consumption.

(iv) PRC eliminates thickness build up at high current density areas during current reversal and improves step coverage without pores reaching down to the substrate (Chandrasekar et al. 2008).

3.6.2.2.9 Disadvantages of Pulse and Pulse Reverse Techniques. The disadvantages of pulse current and pulse reverse technique, although minimal are:

(i) In most cases, the cost of a pulse rectifier is much greater than a DC unit. It is a highly regulated and sophisticated design that costs more to manufacture.

(ii) The technology requires one to think and plan ahead with a series of procedures to follow in order to obtain the best results.

(iii) For the chemical manufacturers, the requirement for additives is reduced.

3.6.2.2.10 Technological Applications. Pulse plating is used to a large degree for plating on electronic connectors and switch contacts. Less stressed pulse plated deposits made it easy to stamp and form contacts after plating. The economic gains surpass the relatively high cost of pulse power supplies. Manufacturers of semiconductor lead (Pb) frames are using PC to increase the reliability of wire bonds and to enhance deposition rate. High-speed gold and silver-plating solutions specially formulated for pulse deposition are available commercially. In Printed Circuit Boards (PCB) industry, there is a need for miniaturization of high-density interconnections.

The use of PRC for the deposition of copper from acidic electrolytes containing additives, produce enhanced throwing power especially in the holes. Circuit traces can be positioned closer together without shorting one another with the use of pulse technology, for high-density circuitry applications in microelectronics industry (Chandrasekar et al. 2008).

CHAPTER FOUR
EXPERIMENTAL STUDIES

4.1 Purpose

The objective of this study is to fabricate Zn-Al_2O_3, Cr-WC and Cr-SiC composite coatings with the aid of stirrer pomp, magnetic stirrer and air ventilation to suspense the ceramic particles in the electrolyte and consequently to characterize the coating morphologies and to investigate the mechanical properties. Therefore, we draw attention to structural, microstructural and mechanical properties of these composite coatings formed on brass/steel substrates by electrodeposition process. In this context, the coatings were performed by electrodeposition technique. The produced coatings were characterized by X-ray diffractometer (XRD), scanning electron microscope (SEM) including energy dispersive spectroscopy (EDS). Mechanical properties of the coatings were examined by Shimadzu dynamic ultra-micro hardness/micro Vickers hardness test machines for estimating Young's modulus. In addition to mechanical investigation, hardness-depth and load-hardness curves of the layers were obtained to expose ceramic particle effect on mechanical properties in the same conditions.

4.2 Preprocessing

4.2.1 Composition of Bath and Electrodeposition Conditions

4.2.1.1 Zn Baths

In this study, three different electrolytes were described for the composite electrodeposition. The composition of the reference Zn electrolyte *P0* and electrodeposition conditions are shown in Table 4.1. The second and third electrolytes were named as *P5* and *P10*, respectively. The numerical symbols in the bath names represent the Al_2O_3 content of electrolytes for 100 ml solution. The bath codes according to their Al_2O_3 content with average particle diameter about 150 nm are shown in Table 4.2.

Table 4.1 Composition of electrolytes and electrodeposition conditions for P0 coded coatings belong to Zn sets.

Bath composition:	
Zinc chloride (ZnCl):	65 gr/lt
Ammonium chloride (NH_4Cl):	180 gr/lt
Carrier additive:	40 ml/lt
Brightener additive:	3.75 ml/lt
Bath conditions:	
Temperature:	25^oC (room temperature)
pH:	4.8

Table 4.2 Bath codes and sample numbers according to their Al_2O_3 contents and current density conditions.

Electrolyte codes and set names	Al_2O_3 content (gr/100ml)	Current density conditions of the samples (A/dm^2)				
		1	**2**	**3**	**4**	**8**
P0	0	P0-1	P0-2	P0-3	P0-4	P0-8
P5	5	P5-1	P5-2	P5-3	P5-4	P5-8
P10	10	P10-1	P10-2	P10-3	P10-4	P10-8

4.2.1.2 Cr Baths

For this set of the study, three different electrolytes (bath) were described for the composite electrodeposition. The composition of the reference Cr electrolyte (*Bath-Ref.*) and electrodeposition conditions are shown in Table 4.3. The second and third electrolytes were named as *Bath-S* (4 g/100ml SiC addition to the Bath-Ref.) and *Bath-W* (6 g/100ml WC addition to the Bath-Ref.) for SiC and WC additional electrolytes, respectively. The bath codes according to their ceramic content with average particle diameter about 200 nm are shown in Table 4.4. To avoid the precipitation of the ceramic content in the electrolyte, the baths were circulated with magnetic stirrer, air ventilator or both magnetic stirrer and air ventilators.

Table 4.3 Composition of electrolytes and electrodeposition conditions of reference Cr bath.

Bath composition:	
Chromic acid (Cr_2O_3):	300 g/lt
Catalyst:	30 g/lt
Sulfuric-acid (H_2SO_4):	2,18 ml/lt
Gas reducer additive:	6,5 ml/lt
Bath conditions:	
Temperature:	40-50^oC
pH:	-

Table 4.4 Bath codes and sample numbers according to their ceramic contents and frequency conditions.

Electrolyte codes and bath names	Ceramic particle content and type (gr/100ml)	Pulse frequency conditions of the samples (Hz)		
		10	***25***	***50***
Bath-Ref.	0	-	R1	-
Bath-S	4-SiC	S1	S2	S3
Bath-W	4-WC	W1	W2	W3

4.2.2 Preparation of the Substrates

4.2.2.1 Zn Coatings

Cu-35wt%Zn brass plates with an area of 0.5 dm^2 were used as a cathode; a pure Zn plate was used as an anode. Prior to electroplating, the substrates were mechanically polished with 80, 240, 400, 800, 1000 and 2400 grit SiC grinding papers, respectively and then a sequence of cleanings was performed.

4.2.2.2 Cr Coatings

Low carbon steel cylinders with 13 mm diameter and 14 mm length were used as a cathode and Pb-7wt%Sn alloy was used as an anode. Before electroplating, the substrates were mechanically polished with 80, 240, 400, 800, 1000 and 2400 grit SiC grinding papers, respectively and then ultrasonically cleaning step was performed in trichloroethylene for 10 minutes to remove contamination on the

substrate surface. Sequent, etching at 20-30 A/dm^2, in vol%60 H_2SO_4 solution for 1-2 minutes was performed.

4.3 Fabrication of the Coatings and the Schematic Representation of the Electrodeposition Setups

4.3.1 Zn Coatings

In order to suspense submicron sized alumina particles completely, the bath was stirred about 2 h using magnetic stirrer before electrodeposition. The bath codes at which the samples fabricated, the sample codes and the fabrication current densities of the samples are shown in Table 4.2. Figure 4.1 represents the electrodeposition setup for all deposition *sets P0, P5* and *P10*. These sets are called with the same name of the electrolytes where they fabricated. Several samples were obtained at different current densities in these three bath conditions.

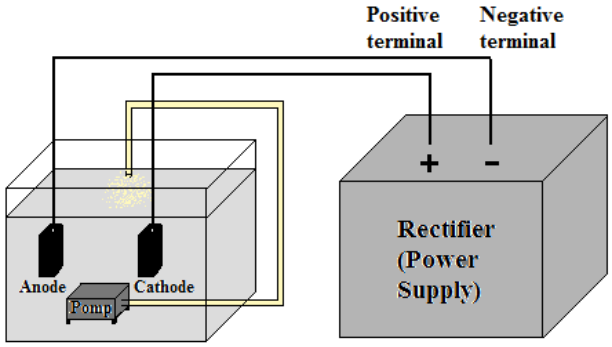

Figure 4.1 Schematic representations of the experimental setup for Al_2O_3 reinforced Zn matrix composite coatings.

4.3.2 Cr Coatings

Optimization studies for this set were firstly performed in a polymer cell with the aid of magnetic stirrer to suspense submicron sized ceramic particles but it was decided to change the stirring type to suspense the particles completely in order to discourage the precipitation problem. After this, the coatings were fabricated in a glass cell in dimensions 200 mm length, 100 mm width and bearing three air

channels for air circulator pumps. One channel from the anode side was disabled to make a particle dense region in front of the cathode (steel substrate) and magnetic stirring was continued simultaneously. Figure 4.2 represents the schema of the experimental setup where Cr matrix coatings were fabricated.

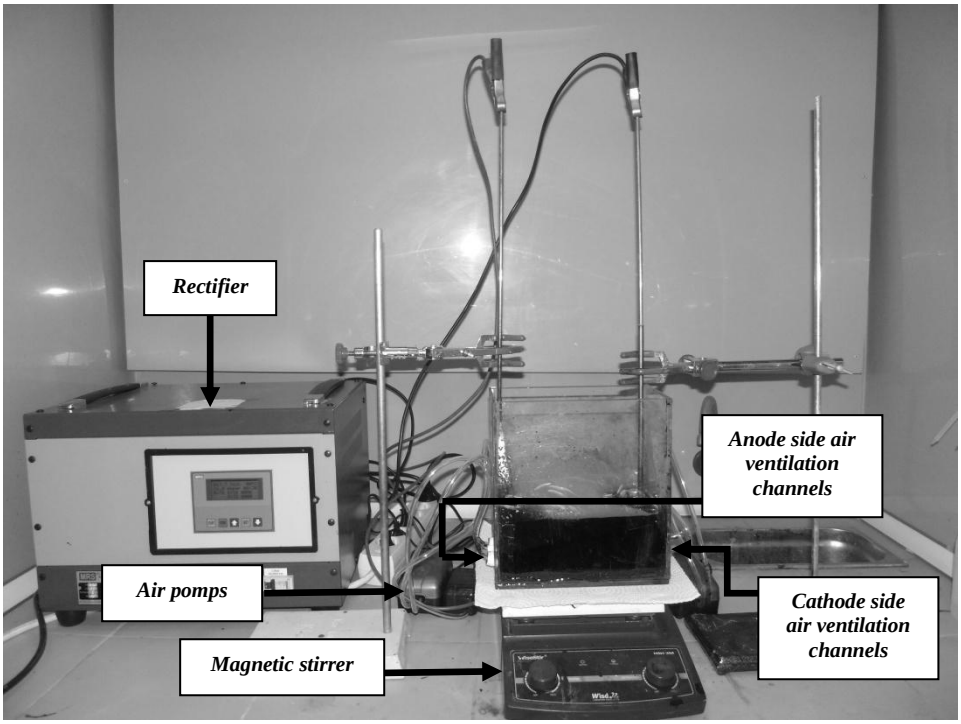

Figure 4.2 Schematic representation of the experimental setup for Cr matrix composite coatings.

a) Optimization studies

In first step of optimization studies, the current density effect was examined. While it is known in industrial applications 50-60 A/dm^2 is optimum values, the coatings for this set were fabricated in parameters such as 50 and 60 A/dm^2. As a result of morphological and mechanical observations the ideal current density was chosen as 60 A/dm^2.

In second step, favorable agitation type was fixed. For this optimization step, magnetic stirring and air ventilation with simultaneously magnetic stirring types and their effects on the morphology of the composite structures were compared. Because of the increased deposition quantity, advanced surface morphology and decreased

agglomeration and particle precipitation, second type of agitation was chosen as optimum parameter for all experimental studies.

Lastly, the effect of current type was examined. For this fabrication set, only the current type was changed (DC: *direct current* – PC: *pulse current*) and the other parameters were adopted as constant. Depending on the mechanical test results and surface morphologies, PC was chosen as an ideal current type to fabricate the composite coatings with advanced properties.

As a result of these optimization sets, optimum parameters were found to be *60 A/dm^2*, *air ventilation and magnetic stirring simultaneously* and *PC* chosen for current density, agitation type and current type, respectively. In addition to this, another set was fabricated for four different frequency conditions in pulse current to compare its effect on the properties.

b) Systematic studies

Systematic studies were carried out for different combinations of the detailed parameter in optimization studies section. These parameters for the all sets were given in Table 4.5 and 4.6.

Table 4.5 The coatings fabricated with DC.

DC (time : 40 minutes)	
1.	No particle addition, Magnetic stirring, 50 Ampere
2.	No particle addition, Magnetic stirring, 60 Ampere
3.	No particle addition, Magnetic stirring & air ventilation, 60 Ampere

Table 4.6 The coatings fabricated with PC.

PC ($I_{avr.}$ = 60 A/dm^2, Magnetic stirring & air ventilation, time : 40 minutes)			
1.	No particle addition, f= 25 Hz		
2.	SiC, f=10 Hz	***5.***	WC, f=10 Hz
3.	SiC, f=25 Hz	***6.***	WC, f=25 Hz
4.	SiC, f=50 Hz	***7.***	WC, f=50 Hz

Calculation of the pulse current parameters:

As a function of T_{on} and T_{off}, one of the pulse current parameters and frequency, were calculated as detailed below:

- **for f = 10 Hz;**

  T_{on} = 80 ms T_{off} = 20 ms

$$f = \frac{1}{T_{ON} + T_{OFF}} = \frac{1}{T} \quad f = \frac{1}{80 + 20} = 0{,}01\ ms = 10\ Hz$$

$$\gamma = \frac{T_{ON}}{T_{ON} + T_{OFF}} \quad \gamma = \frac{80}{80 + 20} = 0{,}8$$

$I_{avr.}$ = peak current density (I_P) x work time (γ)

$$60 = I_p \times 0{,}8 \quad \Rightarrow I_p = 75\ A/dm^2$$

- **for f = 25 Hz;**

  T_{on} = 20 ms T_{off} = 20 ms

$$f = \frac{1}{T_{ON} + T_{OFF}} = \frac{1}{T} \quad f = \frac{1}{20 + 20} = 0{,}025 ms = \ 25\ Hz$$

$$\gamma = \frac{T_{ON}}{T_{ON} + T_{OFF}} \quad \gamma = \frac{20}{20 + 20} = 0{,}5$$

$I_{avr.}$ = peak current density (I_P) x work time (γ)

$$60 = I_p \times 0{,}8 \quad \Rightarrow I_p = 120\ A/dm^2$$

- **for f = 50 Hz;**

  T_{on} = 15 ms T_{off} = 5 ms

$$f = \frac{1}{T_{ON} + T_{OFF}} = \frac{1}{T} \quad f = \frac{1}{15 + 5} = 0{,}05\ ms = \ 50\ Hz$$

$$\gamma = \frac{T_{ON}}{T_{ON} + T_{OFF}} \quad \gamma = \frac{15}{15+5} = 0{,}75$$

$I_{avr.}$ = peak current density (I_P) x work time (γ)

$$60 = I_p \times 0{,}75 \quad \Rightarrow I_p = 80\, A/dm^2$$

Table 4.7 Pulse current parameters for electrodeposition.

Frequency (Hz)	***Pulse-base time (ms) Work time (%)***			***Current density (A/dm^2)***	
	T_{on}	***T_{off}***	***ν***	***Peak***	***Average***
10	80	20	0,8	75	60
25	20	20	0,5	120	60
50	15	5	0,75	80	60

4.4 Characterization

4.4.1 pH Measurement

After preparation of the solutions, pH values of the solutions were measured to determine their acidic and basis characteristics using a standard pH meter with Mettler Tolede electrode.

4.4.2 X-Ray Diffractions (XRD)

X-ray diffraction (XRD) patterns of electrodeposited composite coatings were determined by means of multipurpose Rigaku D/Max-2200/PC Model diffractometer with a Cu K_α radiation by using multipurpose thin film attachment. Measurements were performed by applying 40 kV voltages and 36 mA current.

4.4.3 Scanning Electron Microscopy (SEM) / Energy Dispersive Spectroscopy (EDS)

The surface morphologies of both substrates and coatings were examined by a Scanning Electron Microscope (JEOL-JSM 6060 SEM) with an Energy Dispersive

X-ray spectroscopy (IXRF System EDS) system attachment. Accelerating voltage of 20 kV was used for the SEM imaging and SEM/EDX analyses. Weight percentage distributions and X-ray mapping of elements were determined by EDS.

4.4.4 Nano Indentation Dynamic Ultra Micro-Hardness (DUH)

The indentation studies of composite coatings includes determination of *hardness, elastic modulus and % elastic recovery rate (ERR)* were performed using nano indenter. Shimadzu DUH-W201, DUH-W201S model Dynamic Micro-Hardness Tester was used for indentation tests with a working range 0,1 – 1961 mN. In this study, all the hardness tests were realized under 25 mN applied load and average values of three indentation results were given with an error factor %10 in the figures.

4.4.5 Micro-Vickers

Shimadzu HMV-2 model Micro-Hardness Tester was used for hardness tests with a working range 98,07 mN ($HV_{0,1}$) - 19.614 N (HV_2). In this study, all the hardness tests were realized under 980,7 mN applied load.

CHAPTER FIVE
RESULTS AND DISCUSSION

Anti-corrosion coatings fabricated by electrodeposition have been widely researched (Limin et al. & Vaskevich et al. 2005). With the appearance of nano ceramic particles, nano composite electrodeposition has been paid more attention for its potential applications in improving corrosion resistance (Benea et al. 2002, Yunying et al. 2004 & Fangzu et al. 2004). For example, Benea et al. (2002) reported that nano SiC particles in the Ni-SiC composite coating decreased both the electrochemical corrosion and the wear corrosion, compared with the pure nickel coating. Fangzu et al. (2004) examined the anticorrosion properties of Zn-Fe-SiO_2 composite coating in the neutral solution, and the results indicated that the corrosion resistance was improved by increasing the content of SiO_2. Zn-Ni alloy has been widely applied as highly corrosion resistant coating, especially in the automobile industry (Gavrila et al. 2000 & Lehman et al. 2002). The α-Al_2O_3/SiC/WC possesses excellent chemical stability and good mechanical properties, such as high micro hardness and wear resistance. It has been used extensively in metal matrix composite coatings (Wu et al. 2004, Alirezaei et el. 2004, Lee et al. 1988 & Shrestha et al. 2004). In our present work, the method of fabricating the hard, wear resistant Zn-Al_2O_3 / Cr-SiC / Cr-WC coatings have been determined. The aim of the present study is to reveal the coating process, analyses the co-deposited products, furthermore investigate the mechanical behaviors.

In this part of the study, characterization of the coating morphologies and the investigation of the mechanical properties were performed. Therefore, we draw attention to microstructural and mechanical properties of Zn-Al_2O_3 composite coatings formed on brass substrates and Cr-SiC/Cr-WC composite coatings formed on steel substrates by electro-deposition process. The produced coatings were characterized by X-ray diffractometer (XRD), scanning electron microscope (SEM) including energy dispersive spectroscopy (EDS). Mechanical properties of the Zn matrix coatings were examined by Shimadzu Dynamic Ultra-micro Hardness Test machine for estimating young's modulus due to load-unload sensing analysis, in addition to mechanical investigation hardness-depth and load-hardness curves of the

layer was obtained to expose Al_2O_3 effect on mechanical properties in the same condition and the Cr matrix coatings were examined by Shimadzu Micro Hardness Test machine to expose SiC/WC effect on mechanical properties in the same condition such as pulse current frequency.

5.1 Phase Analysis

5.1.1 Phase Analysis for Zn Matrix Composite Coatings

The phase identifications of coatings were performed by means of XRD technique for all samples fabricated using electrodeposition system. Figure 5.1 denotes XRD patterns of Al_2O_3 powder and coated samples chosen from sets such as P0, P5 and P10.

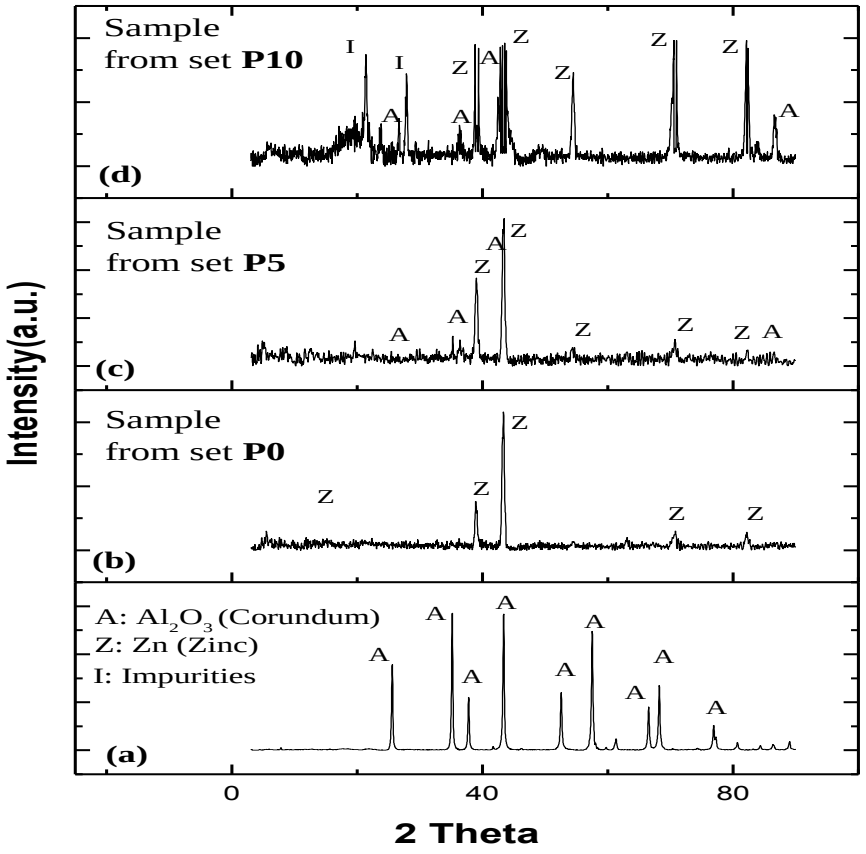

Figure 5.1 XRD patterns of (a) co-deposited alumina powder and samples chosen from set (b) P0, (c) P5, and (d) P10.

As it can be seen in this figure, pure Al_2O_3 powder contains only one phase structure, corundum. Similarly, metallic phase structure is shown in Figure 5.1 for Zn coating fabricated in electrolyte P0. Nevertheless, from the other two patterns for the samples fabricated in electrolyte P5 and P10, it is clearly shown that sub-micron sized alumina ceramic powders are successfully co-deposited with no chemical interaction.

5.1.2 Phase Analysis for Cr Matrix Composite Coatings

The phase identifications of coatings were performed by means of XRD technique for all Cr matrix composite coatings. Figure 5.2 shows the XRD patterns of pure Cr coatings, samples chosen from SiC reinforced composite coatings, and WC reinforced composite coatings, respectively.

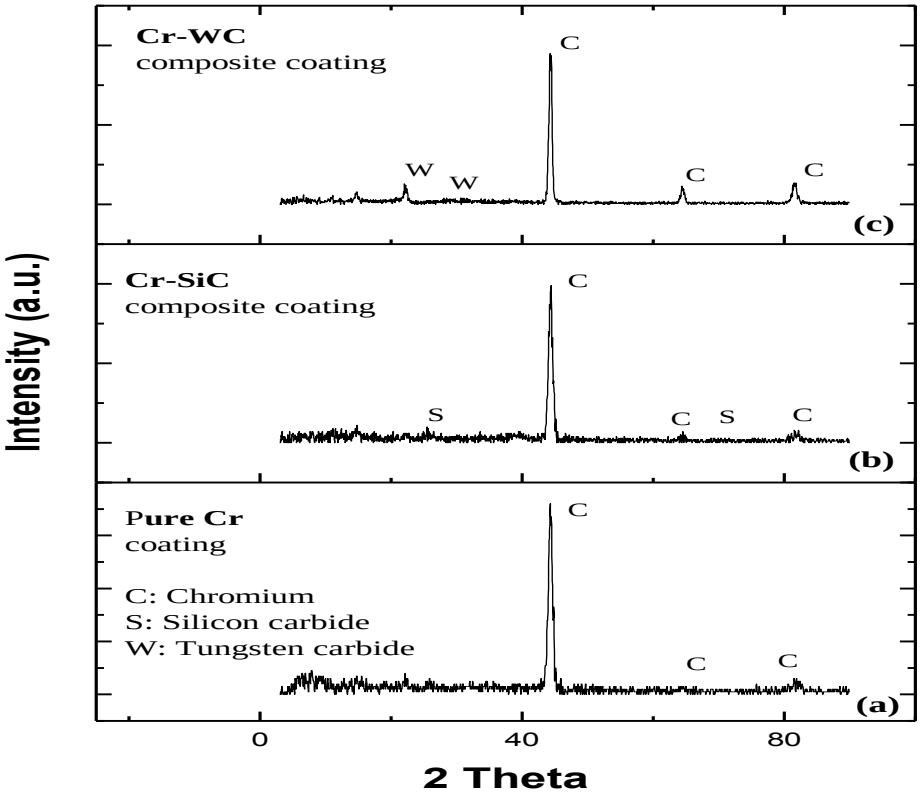

Figure 5.2 XRD patterns of (a) pure Cr coatings, (b) samples chosen from SiC reinforced composite coatings, and (c) WC reinforced composite coatings.

As it can be seen in Figure 5.1.a, coatings, fabricated in reference chromium bath, contains only metallic Cr phase structure. Nevertheless, from the patterns belong to the coatings fabricated in SiC and WC additional baths, it is clearly seen that the co-deposition process was successfully occurred with no chemical interaction between electrolyte and the particles (see Figure 5.2.b and 5.2.c for details).

5.2 Microstructure

5.2.1 SEM Results for Zn Matrix Composite Coatings

It is clearly shown in the SEM images of the coatings that the morphological structures of samples are closely the same for all coatings fabricated in the same sets. Figures 5.a, 5.b and 5.c represent the SEM morphologies and map analyses of the samples chosen from the sets P0, P5 and P10, respectively. The surface image of sample chosen from set P0 (see Figure 5.a) shows homogenous and non-porous characteristics and it is similar for Zn and O map analyze results for the same sample. However, for the samples related with set P5 and P10, Figures 5.b and 5.c, demonstrate partial homogenous structures. To the extent that map analyzes of element Al and O can be observed. In this case, Al_2O_3 particles were homogenously distributed in Zn coating. In addition SEM morphologies of samples including *P5-3*, and *P5-4* are given in Figures 5.4.a and 5.4.b, respectively. In these figures, embedded and Zn coated particles can be seen in details. Similar results can be seen elsewhere (Stroumbouli,2005).

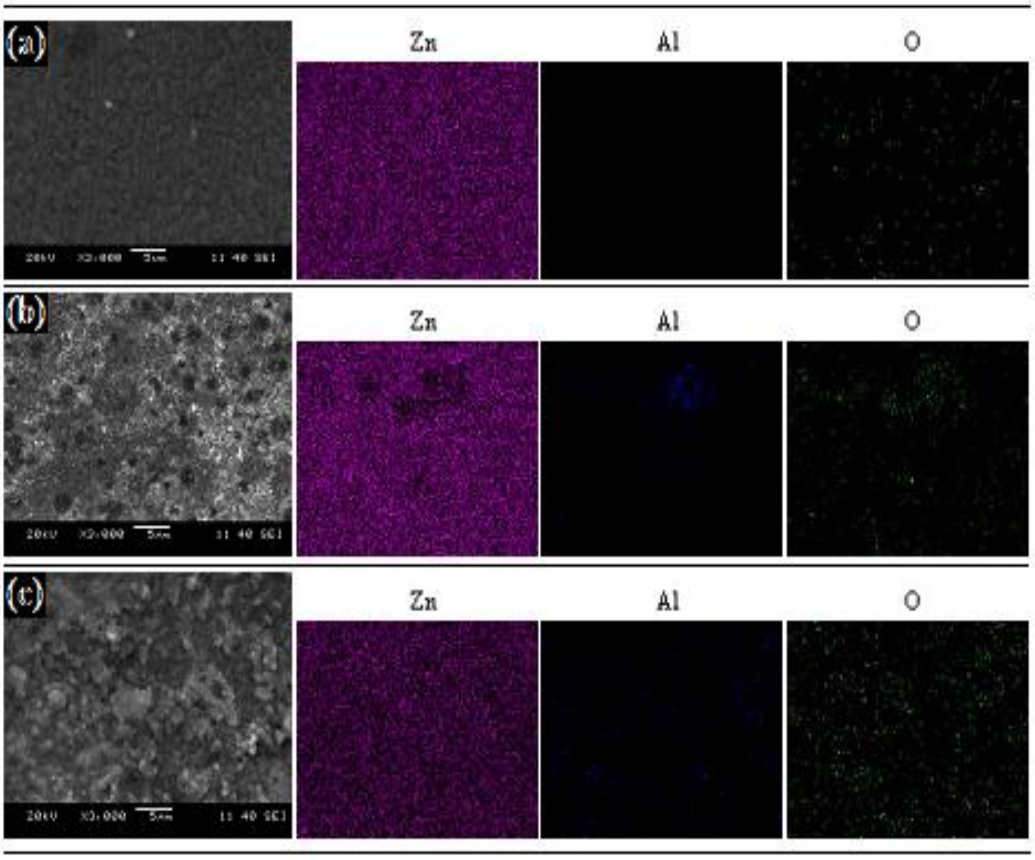

Figure 5.3 SEM morphologies and map analysis of samples chosen from set (a) P0, (b) P5 and (c) P10, respectively.

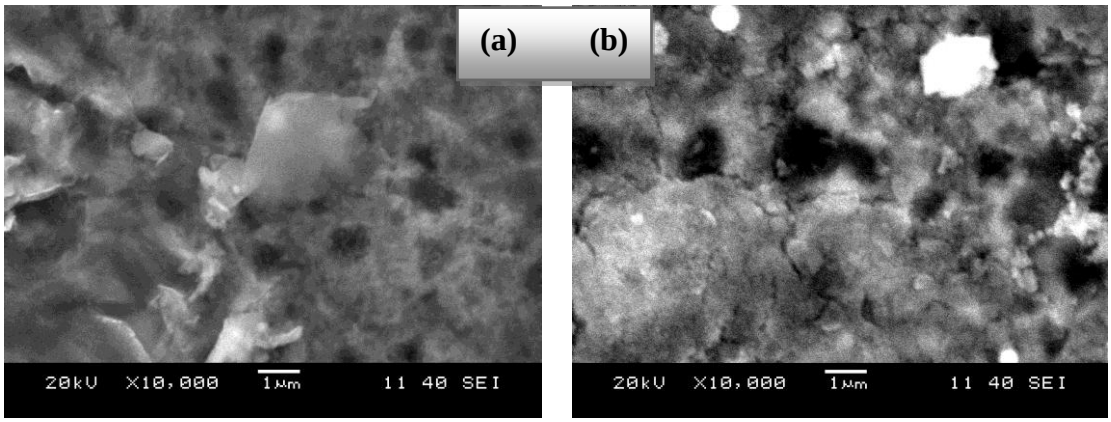

Figure 5.4 SEM morphologies of samples (a) *P5-3*, and (b) *P5-4*, respectively.

5.2.2 SEM Results for Cr Matrix Composite Coatings

5.2.2.1 Optimization

Optimization studies were performed for agitation type, current density and current type parameters in electrodepositing system.

5.2.2.1.1 Current Density. It is known that the ideal current density for industrial applications is approximately 50-60 A/dm^2. With the shore of commentaries explained above, for two different current densities 50 and 60 A/dm^2 with DC, optimization studies was carried out for current density optimization.

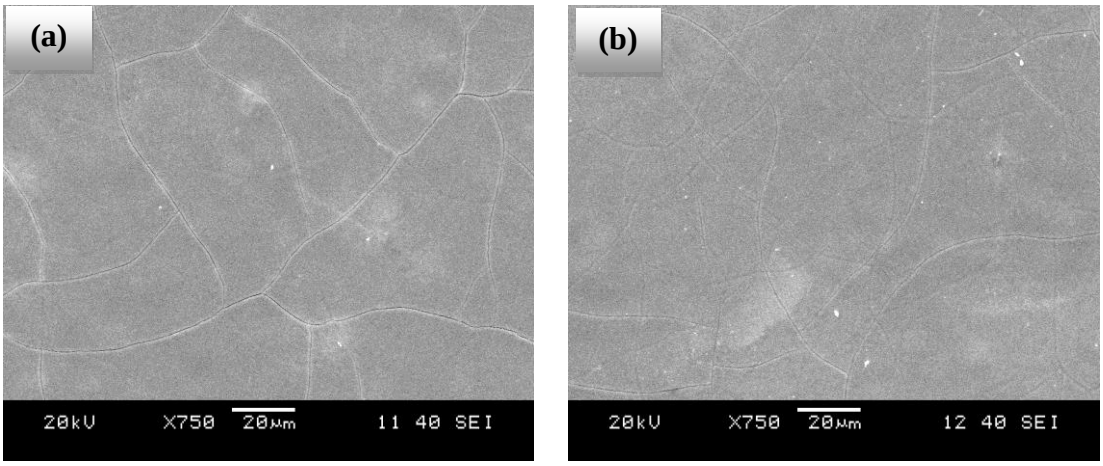

Figure 5.5 SEM micrographs of Cr matrix composite coatings produced using current densities such as (a) 50 A/dm^2 DC, and (b) 60 A/dm^2 DC.

When the SEM images of Cr matrix composite coatings produced using current densities such as 50 A/dm^2 DC, and 60 A/dm^2 DC given in Figure 5.5.a and 5.5.b were viewed, it was seen that the morphological structures were approximately the same for each condition. The reason for the surface cracks seen in these images is thought to be the uncontrolled parameter temperature during deposition.

The coatings fabricated in higher current density conditions show that mechanical properties are improved depending on their decreased grain sizes. However, for industrial applications it is possible to coat the surfaces in shorter times for higher

current densities. For these reasons, current density with 60 A/dm^2 was chosen as optimum current density parameter.

5.2.2.1.2 Agitation Type. This part of the study was performed on agitation types, such as magnetic stirring and air ventilation with simultaneously magnetic stirring to obtain homogenous ionic concentration in the electrolyte and to circulate the suspension containing ceramic particles.

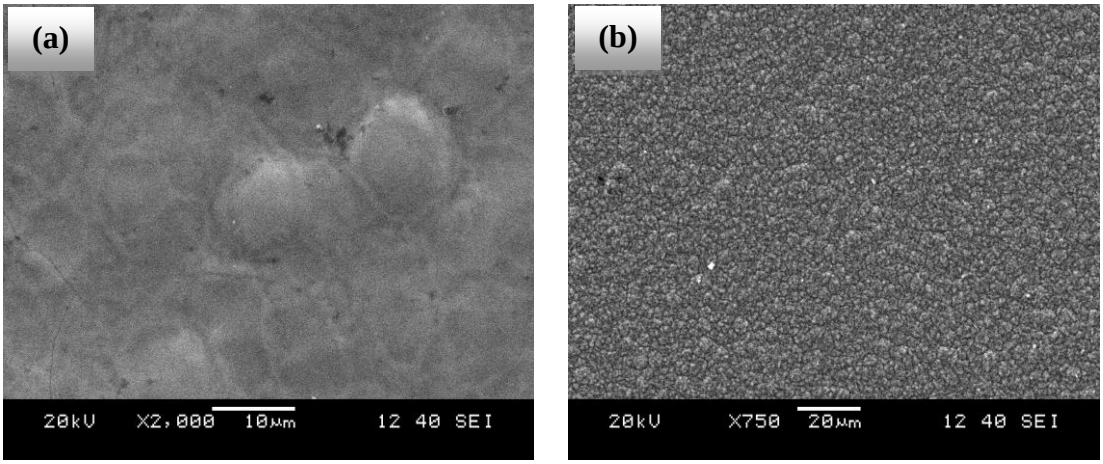

Figure 5.6 SEM micrographs of Cr matrix composite coatings produced using (a) magnetic stirring and (b) air ventilation with magnetic stirring under 60A/dm^{2}current density.

The visual results of composite coatings for these two different parameters were given in Figure 5.6. As seen in Figure 5.6.b, magnetic stirring and simultaneously air ventilation improve the surface quality and decreases the grain size of the coating. With the correlation of grain size and mechanical properties -when grain size decreases hardness increases- optimum agitation type was chosen as magnetic stirring and simultaneously air ventilation. In addition to this, an advantage of this agitation type was found as controllable temperature parameter. External air circulation keeps the bath temperature in lower levels when higher current densities increase it.

5.2.2.1.3 Current Type. The coatings were fabricated using pulse current (PC) as an alternative current type for direct current (DC).

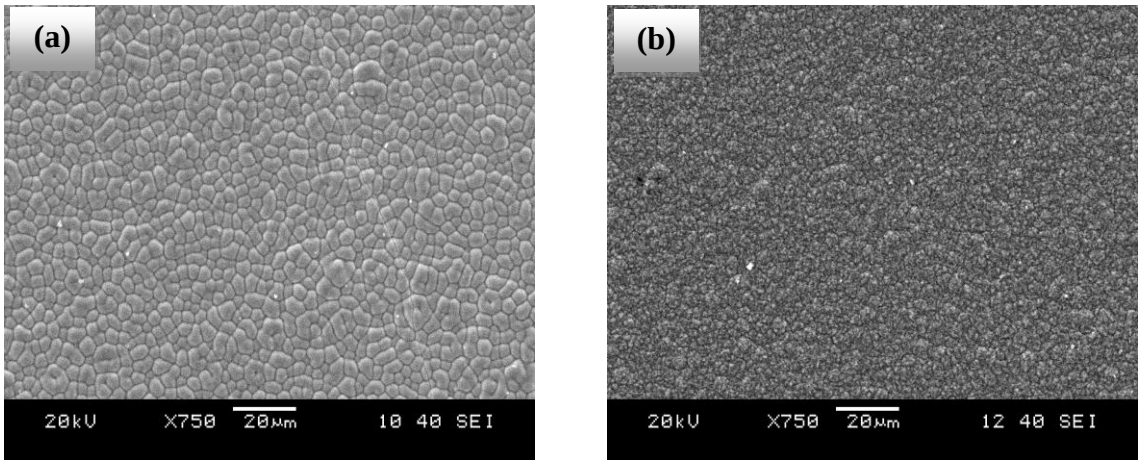

Figure 5.7 SEM micrographs of Cr coatings produced using (a) DC and (b) PC.

For some cases, PC gives advanced properties to nanocomposite coatings than DC. The similar effects were reported by Low et al., (2005). These advanced properties can be listed such as surface microstructure (Figure 5.4) and increased co-deposition rate of ceramics with metal matrix.

5.2.2.2 Results for Systematic Studies

These studies were observed in two sub-groups coatings containing SiC and WC ceramic particles. The aim for this group studies was observation of particle type and pulse frequency effect on morphological and mechanical properties of the composite coatings.

SEM images belong to systematic studies interpreted based on the particle type and pulse frequency effect on the coating structures. Figures 5.8.b, 5.8.c, and 5.8.d shows the SEM images according to increased frequencies. When the images are compared with each other, a small decrease in the grain size with increased frequency can be seen easily. Similarly, from the images in Figures 5.8.e, 5.8.f, and 5.8.g for Cr-WC coatings, with increased frequency the grain size decreases and grains show leaf-shaped structures.

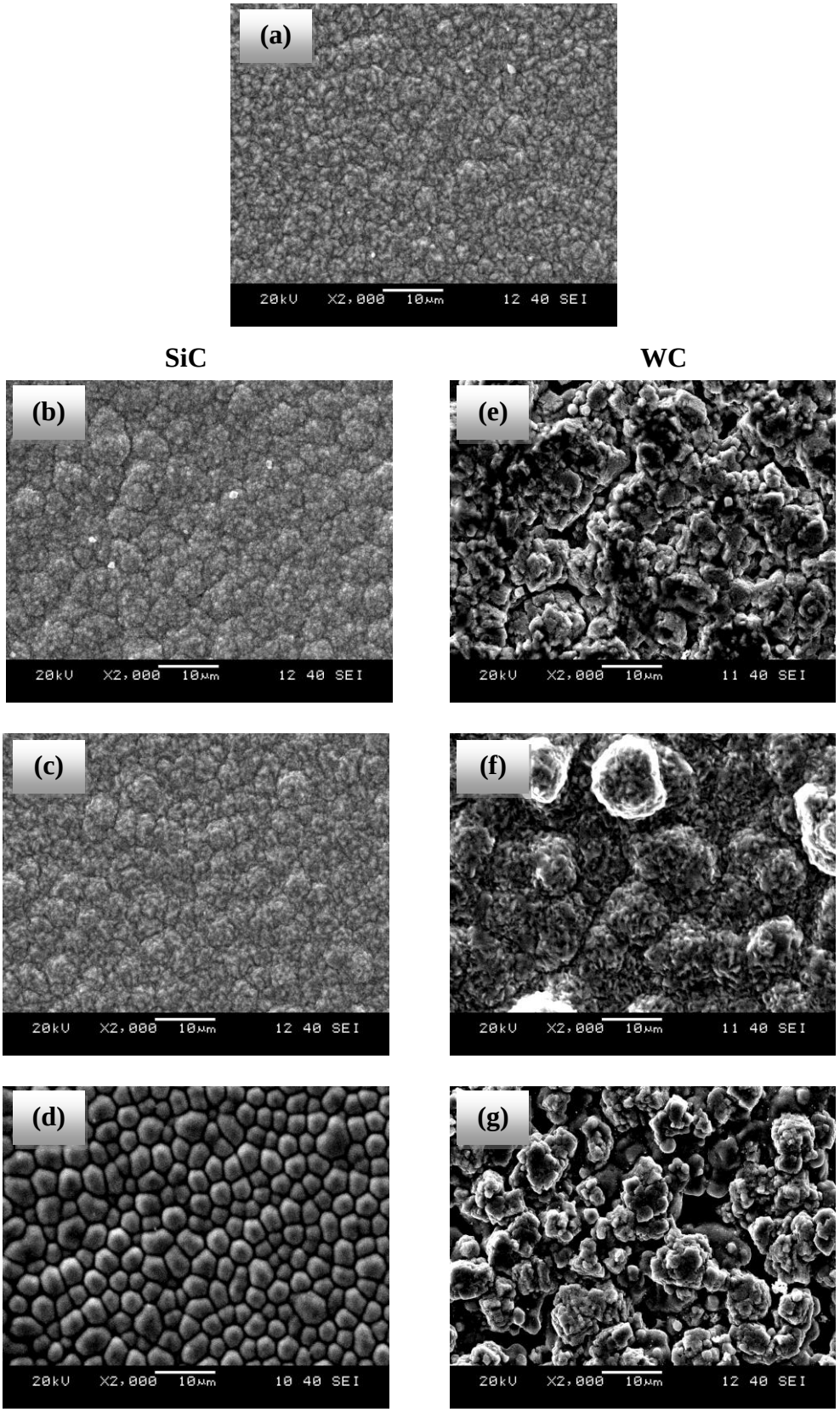

Figure 5.8 SEM images belong to (a) R1, (b) S1, (c) S2, (d) S3, (e) W1,(f) W2 and (g) W3 coded samples. Embedded and metal coated agglomerates of the ceramic particles at x2000 magnification.

After this, to compare the effect of particle addition and particle type on the morphologies, the coatings were fabricated in same frequency conditions and then Cr (reference coating), Cr-SiC and Cr-WC coatings were examined using SEM as shown in Figures 5.8.a, 5.8.c, and 5.8.d. The obtained results showed that, the reference coating has finer grain structure to the extent that SiC and WC reinforced Cr composite coatings have coarser grain structures.

Nonetheless, map analyzes results in Figures 5.9.a, and 5.9.b figured out that sub-micron sized SiC and WC ceramic particles were co-deposited with Cr successfully. Even though it was thought that the surface morphologies were homogenous, when all the coated surfaces were inspected, it can be easily seen from map analyze results that there were non-homogenous parts on the surfaces.

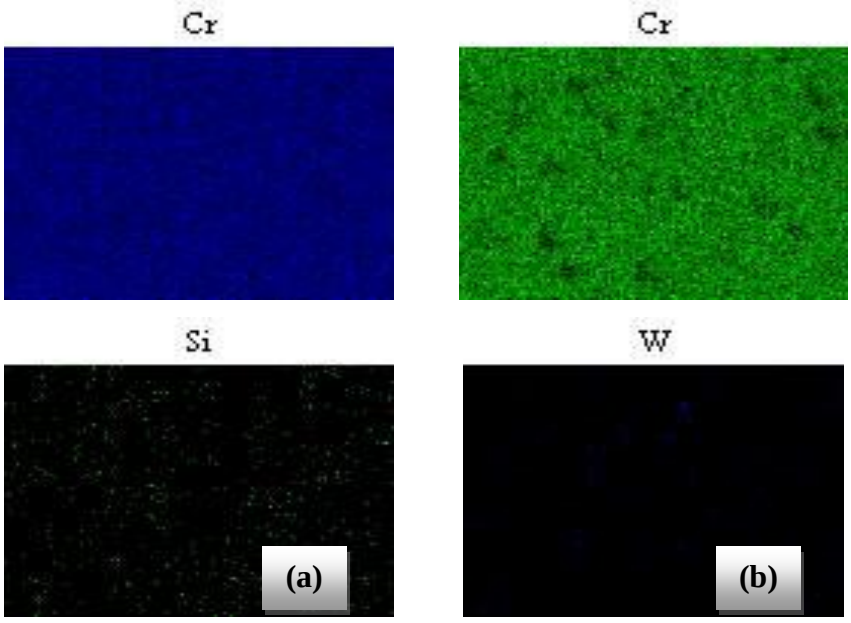

Figure 5.9 Map analyzes results of (a) SiC reinforced and (b) WC reinforced Cr coatings.

5.3 Mechanical Properties

5.3.1 DUH (Dynamic Ultra Micro Hardness) Results

Dynamic ultra micro hardness tests were performed for Zn matrix composite coatings. The indentation studies of samples belong to sets of P0, P5 and P10 includes determination of *hardness, elastic modulus and % elastic recovery rate (ERR)* depending on the increasing current density. Critical area; for analysis in the theory of indentation hardness and applied load are used for hardness determination and elastic modulus are measured from loading-unloading curves of the Zn-Al_2O_3 composite coatings. In addition, % ERRs were calculated from maximum submersion and apparent depth to determine the optimum micromechanical features in terms of production of electrolytic Zn-Al_2O_3 composite coatings. Fabrication parameters, notably the amount of particles, the bath conditions and applied current density are special points to obtain optimum micromechanical properties in coating microstructure.

Indentations results of coatings belong to set P0 are shown in Figure 5.10. Hardness, elastic modulus and % ERRs were examined by increasing current density under 25 mN applied load in details. Average values of three indentation results were given with an error factor %10 in the figures. According to indentation results of these samples in Figure 5.10.a, indentation hardness increased from 0.65 GPa to 1.77 GPa depending on the increasing at current density. This means that when the current density increases without additional particles, the formation of more regular and dense coating microstructures can be obtained. As a result of the loading-unloading curves of the samples in Figure 5.10.b, elastic modulus increased from 28.67 GPa to 66.33 GPa by increasing current density and the % ERRs change from 11.52 % to 13.56 % depending on visible and maximum submersion depth as represented in Figure 5.10.c.

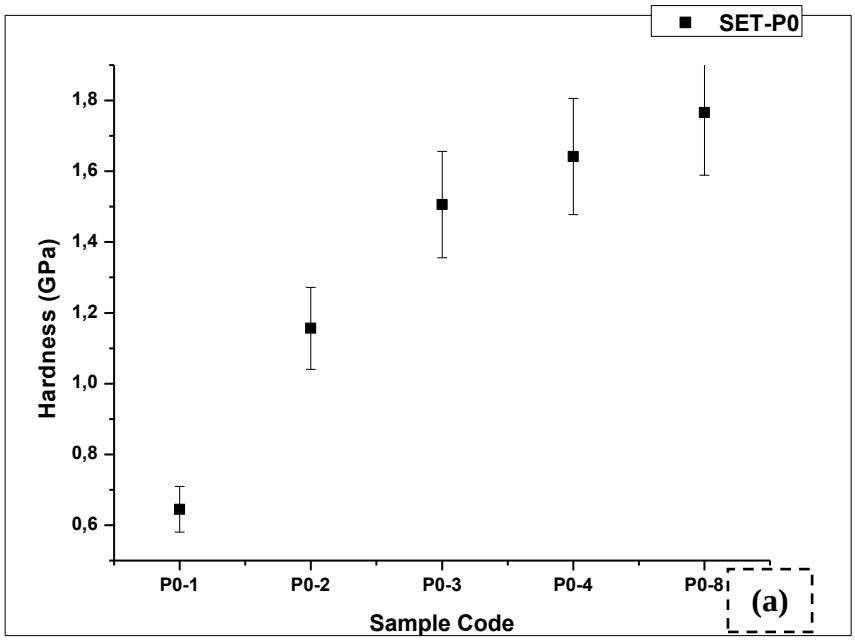
SET-P0
Hardness (GPa)
1,8
1,6
1,4
1,2
1,0
0,8
0,6
P0-1
P0-2
P0-3
P0-4
P0-8
Sample Code
(a)

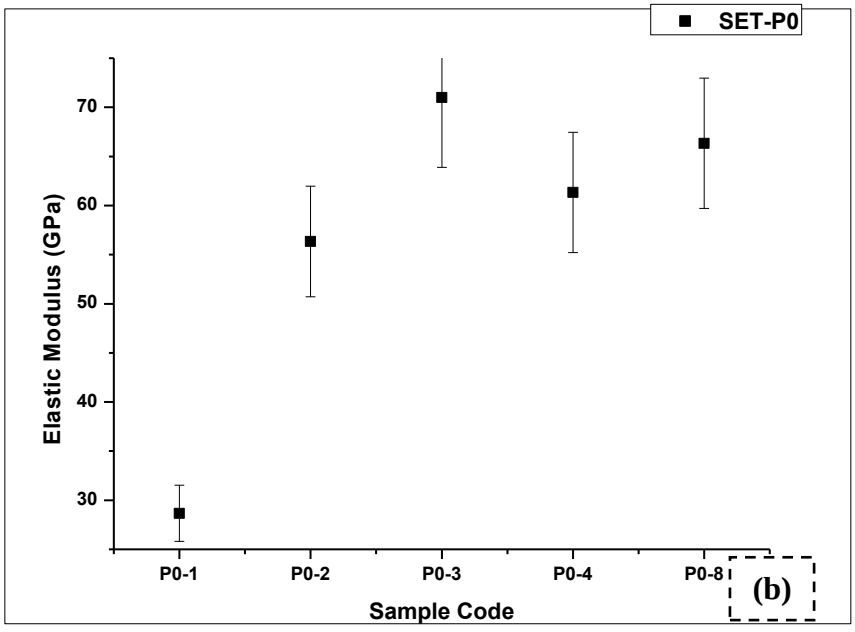
SET-P0
Elastic Modulus (GPa)
70
60
50
40
30
P0-1
P0-2
P0-3
P0-4
P0-8
Sample Code
(b)

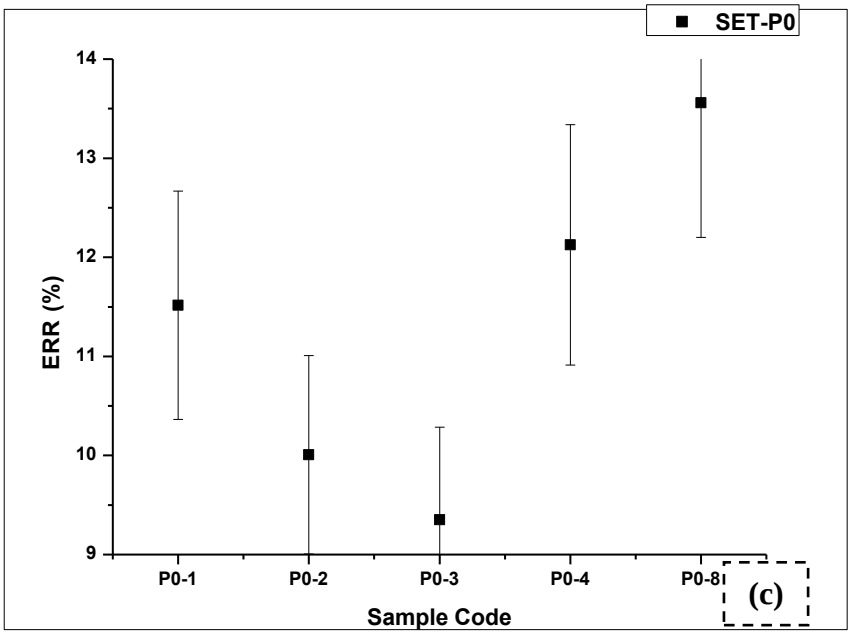

Figure 5.10 (a) Hardness, (b) Elasticity and (c) % ERR variations of P0-coded coatings under 25 mN applied load.

The hardness values of the samples for set P5, depending on the current density, increased from 0.55 to 2.55 GPa as represented in Figure 5.11.a. However, the same increase for the elastic modulus is not possible. As shown in Figure 5.11.b, elastic modulus, which is a micromechanical property of the coatings produced in the bath of P5, changes in the range of 12.67 GPa and 23 GPa. On the analysis of the elastic modulus, depending on the increasing current density, an interesting phenomenon was encountered. To illustrate this, the elastic modulus of sample P5-3 was measured as 56.67 GPa. In this case, the highest elastic modulus value can be expressed by the dense regions caused by particles. Likewise, as seen Figure 5.11.c, % ERR is very high as 69.71% in P0-3 coded sample.

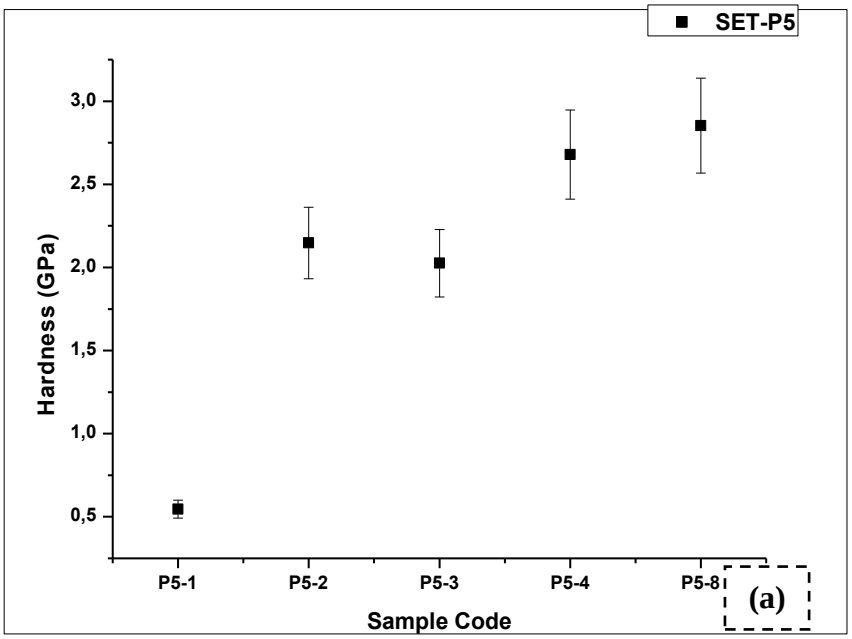
SET-P5
Hardness (GPa)
3,0
2,5
2,0
1,5
1,0
0,5
P5-1
P5-2
P5-3
P5-4
P5-8
Sample Code
(a)

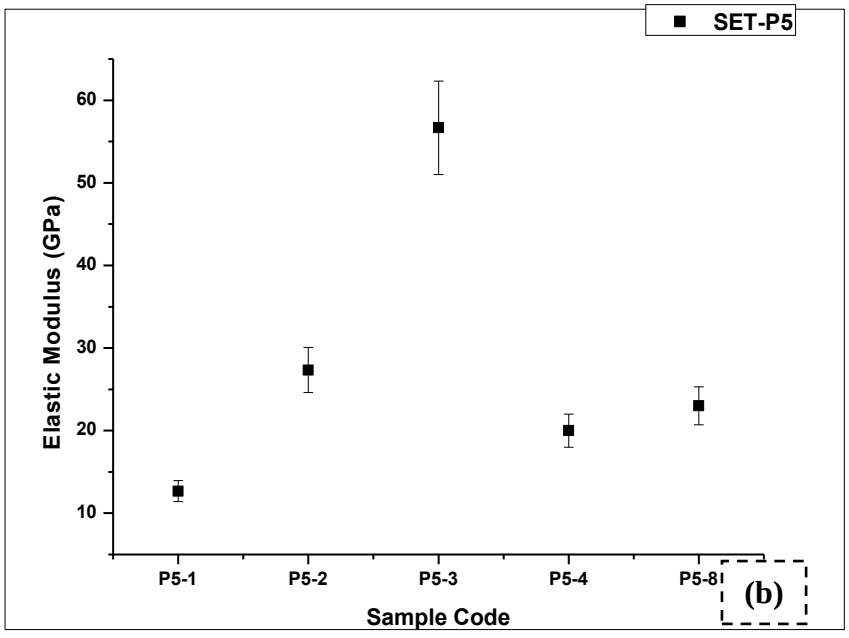
SET-P5
Elastic Modulus (GPa)
60
50
40
30
20
10
P5-1
P5-2
P5-3
P5-4
P5-8
Sample Code
(b)

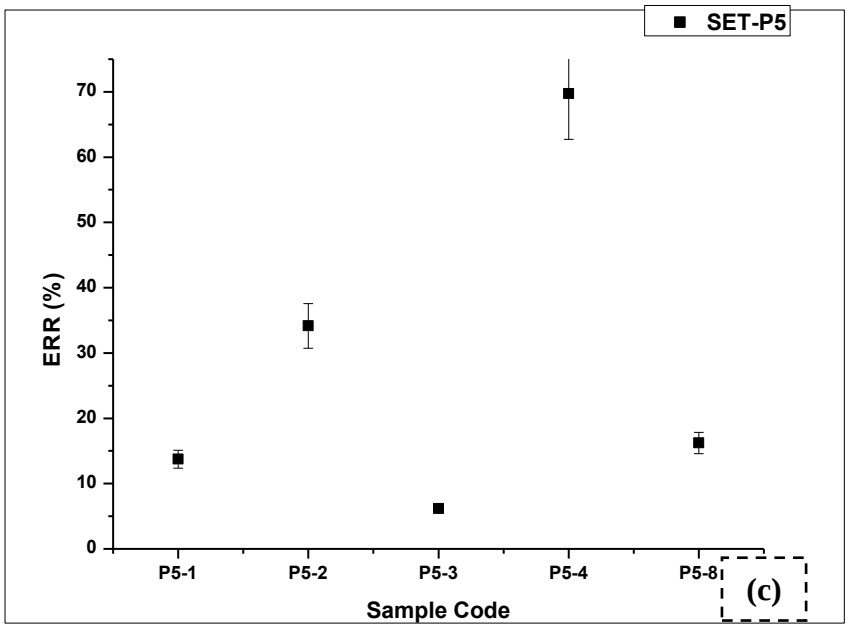

Figure 5.11 (a) Hardness, (b) elasticity and (c) % ERR variations of P5-coded coatings under 25 mN applied load.

The hardness results of P10 coded samples taken from this set denote a change between 1.41 and 1.54 GPa. Especially as represented in Figure 5.12.a, this value shows an increase and has reached to 2.54 GPa for P10-3 coded samples. When the modulus of elasticity results were examined for this set, the increase in these values from 41.33 GPa to 69.33 GPa with linear equation can be seen in Figure 5.12.b. It is clearly seen in Figure 5.12.c that the hardness and % ERR values of the samples change irregularly. The main reason of these irregularities thought to be the increase in the quantity of particles.

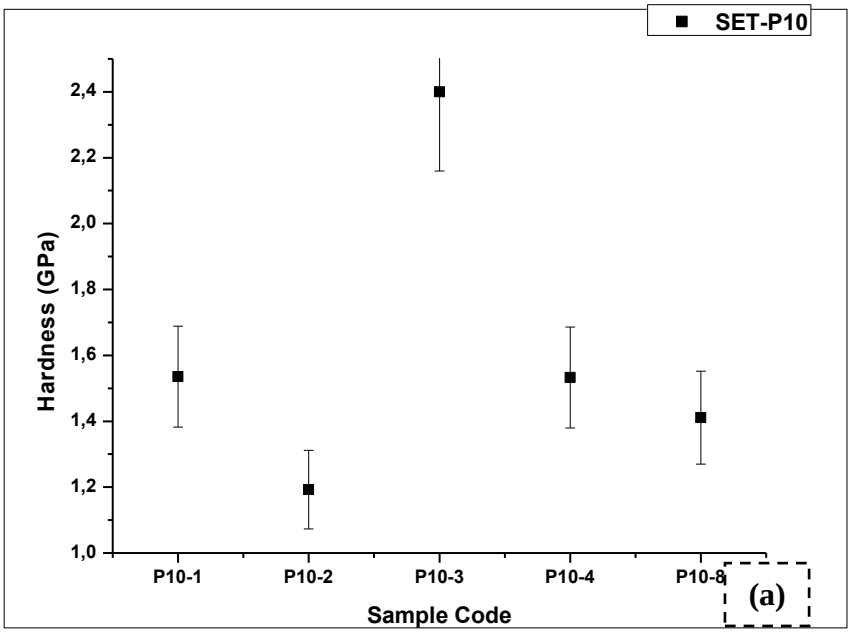
SET-P10
Hardness (GPa)
2,4
2,2
2,0
1,8
1,6
1,4
1,2
1,0
P10-1
P10-2
P10-3
P10-4
P10-8
Sample Code
(a)

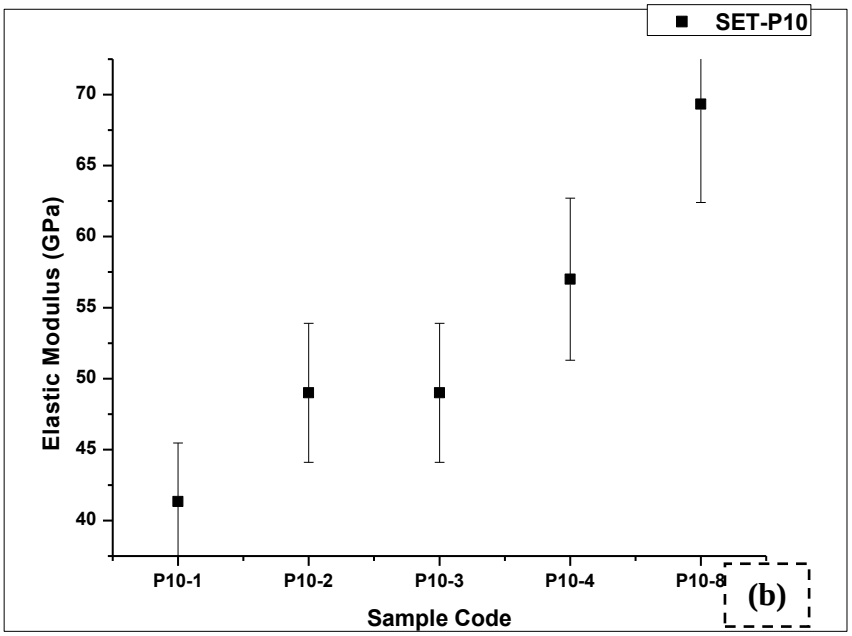
SET-P10
Elastic Modulus (GPa)
70
65
60
55
50
45
40
P10-1
P10-2
P10-3
P10-4
P10-8
Sample Code
(b)

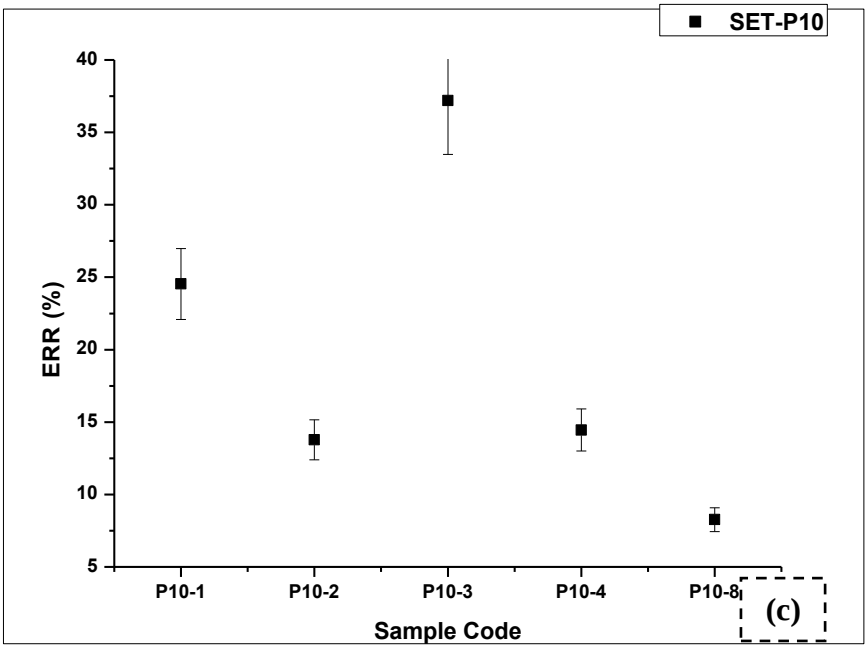

Figure 5.12 (a) Hardness, (b) Elasticity and (c) % ERR variations of P10-coded coatings under 25 mN applied load.

As known, theoretical Vickers Hardness (HV) of coatings can be calculated by indentation parameters such as h_c (critical depth), A_c (critical area) and applied peak load (Uzun, 2005). Table 3 shows the calculated hardness values of P0, P5 and P10 coded coatings under 25 mN applied peak load. It is seen from Table 3 that when current density increased systematically, hardness results of P0-coded samples increased linearly for the same current density and time. On the contrary, hardness of P5 and P10 coded samples changed depending on the amount of additional particles. For instance, hardness curves of P5 and P10 coded samples are shown unexpected behavior owing to existence of particles dense region on the coatings as represented Figure 5.13.a. This condition exposes that coatings with additional particles are harder from P0-coded samples. We have a good agreement with Hou et al. (2002) & Garcia et al. (2001). Nevertheless, the coatings structures are irregular due to deposition conditions. Since the present research is an optimization study, influence of current density and amount of particles to the mechanical properties are being investigated. Garcia et al. (2001) proposed that the best wear resistance was obtained for Ni–SiC composite coatings containing 4–5% rather than 8.5% SiC particle which show increased hardness values.

By the experimentally determined h_c and A_c, the elastic modulus was calculated and the results are listed in Table 3 for different types of Zn and Zn-Al_2O_3 composite coatings. It is clearly seen from Table 3 and Figure 5.13.b that the elastic modulus also exhibits a strong particles and current density dependency. When the current density increases from 1 to 8 A/dm^2, elastic modulus of P0 coded coatings increase and maximum at 3A/dm^2 current density for electrodeposition process. On the other hand, the same condition is seen for P5 and P10 coded coatings. On the particles dense region, elastic modulus values are increased by increasing current density. Meanwhile, when the current density increases from 1 to 3 A/dm^2, elastic modulus of P5 coded coatings are maximum and their values are 49.66, 76.33 and 66.66 GPa under 25 mN applied peak load. On the contrary, when the current density increases from 4 to 8 A/dm^2, additional particles took in consideration and the elastic modulus values change dramatically and show unexpected variations because of irregularity in microstructure of Zn-Al_2O_3 composite coatings.

% ERRs of Zn and Zn-Al_2O_3 composite coatings are changed by current density and additional particles. Notably, it is shown from the Figure 5.13.c, % ERR is minimum under elevated elastic modulus values for each samples.

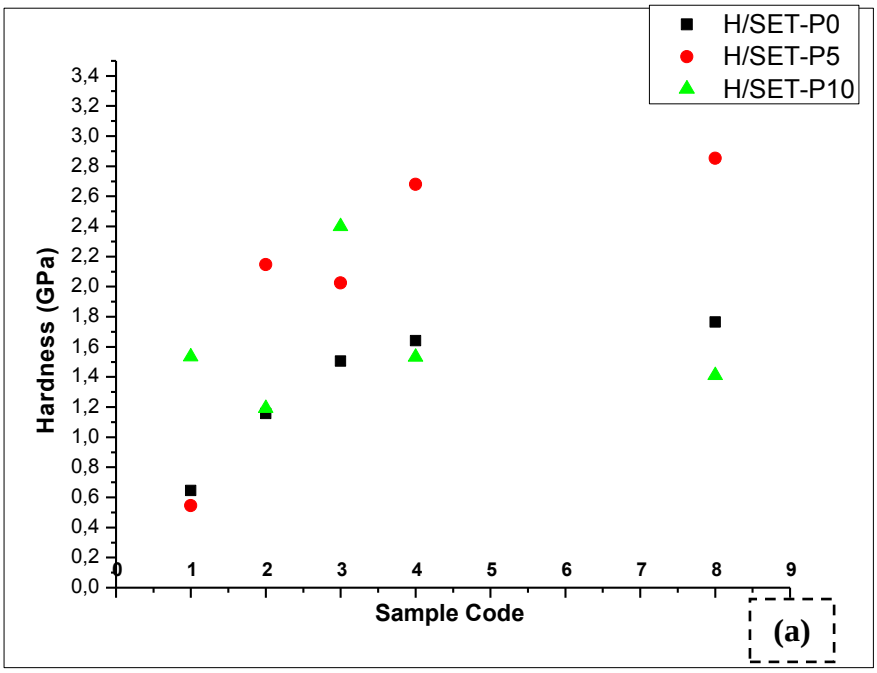

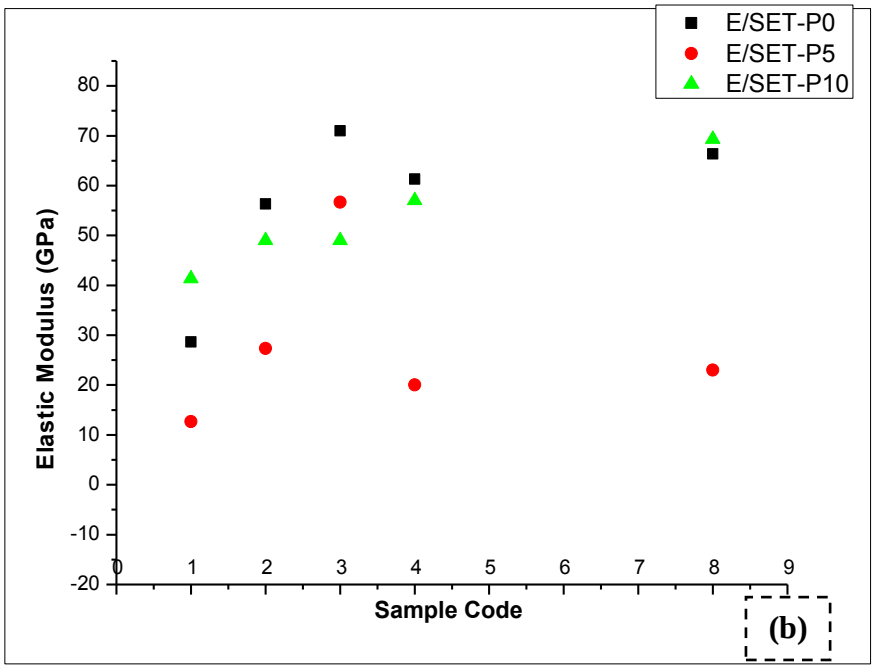

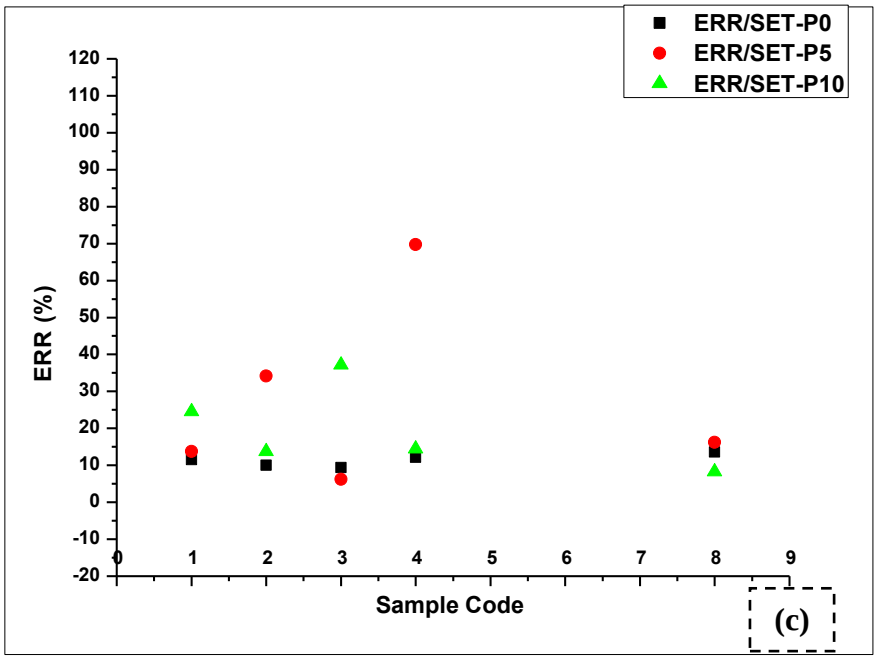

Figure 5.13 (a) Hardness results of P0, P5 and P10-coded coatings, (b) Elastic modulus variations of P0, P5 and P10-coded coatings and (c) % ERR values of P0, P5 and P10-coded coatings depending on current density.

Table 5.1 Indentation results of P0, P5 and P10-coded samples.

Set code	*Sample name*	*Maximum Depth (µm)*	*Critical Depth (µm)*	*Critical Area ($µm^2$)*	*Indentation Hardness (GPa)*	*Young's Modulus (GPa)*	*% ERR*
P0	P0-1	1.366	1.247	41.91	0.65	28.66	11.51
	P0-2	0.996	0.914	22.28	1.16	56.33	10.06
	P0-3	0.862	0.795	16.73	1.51	**71.00**	9.35
	P0-4	0.860	0.779	16.36	1.64	61.33	12.12
	P0-8	0.818	0.737	14.41	1.77	66.33	13.55
P5	P5-1	0.928	0.832	19.95	1.75	49.66	16.50
	P5-2	0.853	0.835	18.48	1.37	76.33	1.86
	P5-3	0.725	0.635	10.69	2.37	**66.66**	15.08
	P5-4	0.764	0.667	11.76	2.13	61.00	15.11
	P5-8	0.841	0.827	18.10	1.38	54.33	3.09
P10	P10-1	0.935	0.786	16.34	1.54	41.33	24.53
	P10-2	1.003	0.908	22.09	1.19	49.00	13.77
	P10-3	0.839	0.698	13.63	2.37	49.00	37.18
	P10-4	0.881	0.786	16.35	1.53	57.00	14.45
	P10-8	0.882	0.820	17.79	1.41	69.33	8.26

5.3.2 Micro Hardness (Vickers) Test Results

Micro-Vickers hardness tests were performed for Cr matrix composite coatings. As known theoretically, decreasing grain size gives the material advanced mechanical properties such as high hardness. But as it seen from the figures, ceramic reinforced composite coatings, which have coarse grains than reference sample, showed better performances in micro-Vickers tests. The main reason for this result is thought to be the effect of embedded ceramic particles with high hardness values. In another word, it was proved that SiC and WC addition showed dominant characteristics than the grain size effect. The obtained hardness results are given in Table 5.2 and Figure 5.14 schematically shows the increase in hardness values for different ceramic addition types according to increasing pulse frequency.

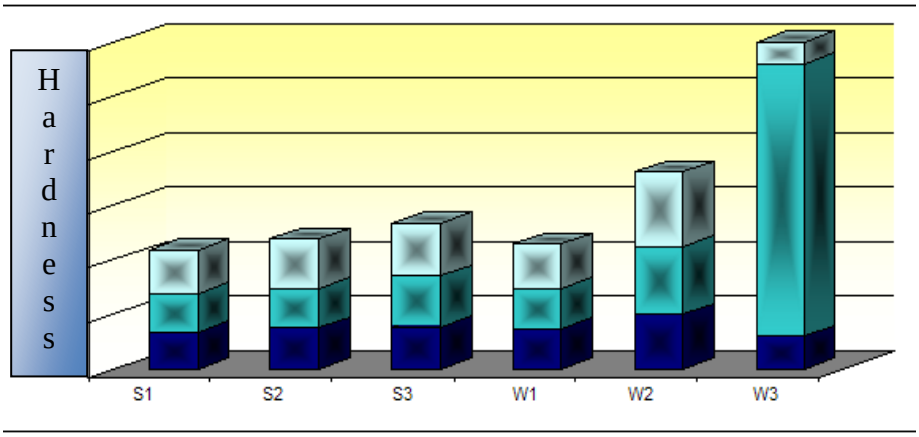

Figure 5.14 Comparable hardness results of systematic studies for R, S, and W-coded samples.

Table 5.2 Hardness ($HV_{0.1}$) results of R, S, and W-coded samples

	R1	***S1***	***S2***	***S3***	***W1***	***W2***	***W3***
1. indentation	561	680	739	785	732	1013	616
2. indentation	592	693	745	937	760	1227	5350
3. indentation	672	811	910	961	790	1361	5998

When the effect of reinforcement type was observed, it was clearly seen that the WC performance was higher than the SiC performance. That was the result that we were waiting depending on the hardness properties of the ceramic particles (Hou et al. 2002).

Another aim of this study was to estimate the wear behavior of the coatings with the shore of obtained hardness results. In a report Luyck and Love (2004) studied on the relationship between the abrasion resistance and the hardness of WC-Co alloys. This research reports hardness and abrasive wear resistance test results from a wide range of WC-Co alloys, varying in cobalt content as well as WC grain size. The results show that the abrasive wear resistance increases with increasing hardness and that the rate of increase is higher for larger WC grain sizes. The increase in abrasive wear resistance was found to be parabolic up to a critical hardness value and exponential above that value. The transition from parabolic to exponential behavior was found to occur at the same contiguity value for all grain sizes, which suggests that at that contiguity value the WC skeleton becomes continuous in all WC-Co

alloys. This study and some others (Lekka et al, 2009) support our study and hypothesis. Some results depict this case are shown in Figure 5.15.

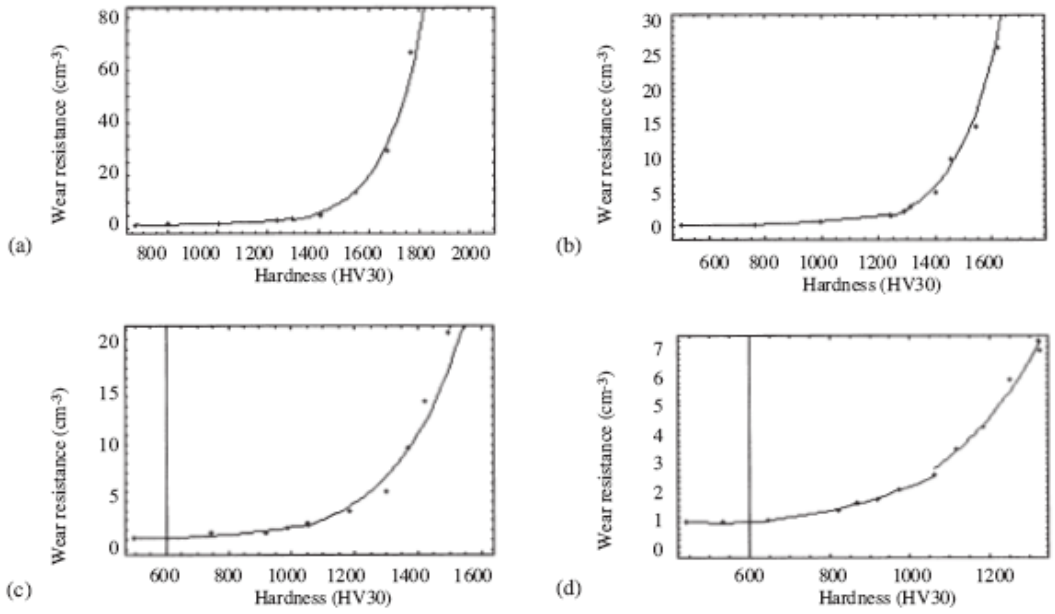

Figure 5.15 Plots of the abrasion resistance versus the hardness of the four groups of WC-Co grades; (a) group *ultra fine*, (b) group *fine*, (c) group *medium*, (d) group *coarse*. The points are the experimental data and the continuous curve sections are the curve sections that best fit the data as determined by a least squares fit.

Another research group studied on corrosion and wear resistant electrodeposited composite coatings and their test results suggest that in the case of pure nickel coating the wear process destroys the nickel oxides passive film so that the underlaying microporous pure nickel layer allows the electrolyte to enter and reach the substrate. In the case of the composite coating the nanoparticles of silicon carbon prevent the total damage of the passive film. The passive film that covers pure nickel coating is composed of two molecular layers of NiO and a molecular layer of $Ni(OH)_2$. The nanoparticles of SiC being much bigger than these layers, but not so big to give rise to the so called chunk effect, are able to protect this film in the way shown in Figure 5.16 (Lekka et al., 2009).

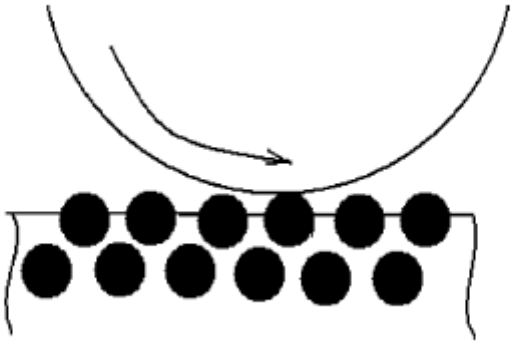

Figure 5.16 Schematic presentation of the influence of the presence of SiC nanoparticles to the coatings' abrasion resistance (Lekka et al., 2009).

-

CHAPTER SIX
CONCLUSION

6.1 General Results

6.1.1 Al_2O_3 Reinforced Zn Composite Coatings

Co-deposition of sub-micron sized Al_2O_3 particles with Zn metal via electrodeposition system was successful. The general results for this process are such as given below:

1) The obtained phase results show that there was no chemical interaction between ceramic particles and the electrolyte. Also it was determined that Al_2O_3 particles were physically absorbed to the cathode surface and made a composite structure with metal Zn.

2) When the SEM images belong to the coatings fabricated in reference and particle additional baths compared coatings with homogenous grain structures can be seen easily. The reason for the partial porous regions on the composite coatings is thought to be the changing bath properties depending on the alumina addition.

3) In high magnifications SEM images and EDS map analyze results support the XRD phase analyzes results and successfully occurred co-deposition process.

4) Based on indentation results of samples for set P0, indentation hardness increased from 0.65 GPa to 1.77 GPa as a function of the increasing at current density. This means that when the current density increases without additional particles, the formation of more regular and dense coating microstructures can be obtained. As a result of the loading-unloading curves of the samples, elastic modulus increased from 28.67 GPa to 66.33 GPa by increasing current density and the % ERRs change from 11.52 % to 13.56 % depending on visible and maximum submersion depth.

5) The hardness values of samples for set P5, depending on the current density, increased from 0.55 to 2.55 GPa. However, the same increase for the modulus of elasticity is not possible. Elastic modulus, which is a micromechanical property of the coatings produced in the bath of P5, changes between 12.67 GPa led to 23 GPa. On the analysis of the elastic modulus, depending on the increasing current density, an interesting situation encountered. To illustrate, the elastic modulus of sample P5-3 was measured as 56.67 GPa. The highest modulus of elasticity value in this case can be expressed by the dense regions caused by particles. Likewise, % ERR is very high as 69.71% in P0-3 coded sample.

6) The hardness results of P10 coded samples taken from this set show a change between 1.41 and 1.54 GPa. Especially, this value shows an increase and has reached to 2.54 GPa for P10-3 coded samples. When the modulus of elasticity results were examined for this set, the increase in these values from 41.33 GPa to 69.33 GPa with linear equation can be seen. It was clearly seen that the hardness and % ERR of the samples change irregularly. The main reason of these irregularities thought to be the increase in the quantity of particles.

7) When the current density increases from 1 to 8 A/dm^2, elastic modulus of P0 coded coatings increase and maximum at 3 A/dm^2 current for electrodeposition process. On the other hand, the same condition is seen for P5 and P10 coded coatings. On the particles dense region, elastic modulus values are increased by increasing current density. Meanwhile, when the current density increases from 1 to 3 A/dm^2, elastic modulus of P5 coded coatings are maximum and their values are 49.66, 76.33 and 66.66 GPa under 25 mN applied peak load. On the contrary, when the current density increases from 4 to 8 A/dm^2, additional particles took in consideration and the elastic modulus values change dramatically and show unexpected variations because of irregularity in microstructure of Zn-Al_2O_3 composite coatings.

6.1.2 SiC/WC Reinforced Cr Composite Coatings

Co-deposition of sub-micron sized ceramic particles such as WC and SiC with Cr metal via electrodeposition system was successful. The general results for this process are as follow:

1) It was seen that the pulse current is an alternative and optimum method for co-deposition of metals with ceramic particles such as Cr-SiC and Cr-WC pairs.

2) As the reason of different co-deposition behaviors of various ceramic additions is thought to be the different physical and electrical properties which they have.

3) The obtained phase results show that there was no chemical interaction between ceramic particles and the electrolyte. Also it was determined that SiC and WC particles were physically absorbed to the cathode surface and made a composite structure with metal Cr.

4) For the sets containing sub-micron sized ceramic particles, the obtained map analyze results show particle dense regions however they show homogenous behavior generally. The extreme hardness values obtained for these two sets are thought to be the hardness results of these dense regions. Nevertheless, map analyzes results support the XRD analysis.

5) When the coatings were compared (coatings with no reinforcement and SiC/WC reinforced), it was seen that the hardness values of the ceramic particle reinforced composite coatings were increased. With respect to the reference coatings, SiC additional composite coatings depict an increased performance close to %50; similarly WC reinforced composite coatings show an increase up to %600 in partial hardness performance.

6) Frequency, as a parameter of pulse current, is decided as an effective parameter on co-deposition of ceramic particles with metals and when the frequency increases the co-deposition performance increases.

6.2 Future Plans

According to all these findings, optimization studies for the coatings with advanced mechanical properties and homogenous structures are planned with changing the several coating parameters. These optimization studies can be performed as detailed below:

1) To obtain the optimum working conditions the present coating system can be modified or to fabricate the coatings with homogenous structures and properties a new parameter controllable system can be designed.

2) Bath circulation system, air ventilation can be modified to obtain homogenous suspensions. In addition to this, cooled air can be used to control the bath temperature and the effect of inert gas (such as Ar and N_2) use on the properties can be researched.

3) The average particle size effect of the additive ceramic particles on the mechanical properties can be studied. In this sense, not only sub-micron sized but also nano sized ceramic particles may be used.

REFERENCES

Ajayan, P.M., Schadler, L.S., & Braun, P.V. (2003). *Nanocomposite Science and Technology,* Weinheim: WILEY-VCH Verlag GmbH Co. KGaA.

Alirezaei S., Monirvaghefi, S. M., & Salehi, M. (2004). Effect of alumina content on surface morphology and hardness of Ni-P-Al_20_3 electroless composite coatings, *Surf. Coat. Technol.*,184, (2-3), 170.

An, M, Zheng, H., & Bian, J. (2006). *Methode of fabricating Zn-Ni-Al_2O_3 composite coating,* China patent: 200610009815.1.

ASM International Handbook Committee. (1994). *Surface Engineering, Volume 5,* (9^{th} ed.), United States of America.

Benea, L. (1998), Composite Electrodeposition-Theory and Practice, Ed: Porto-Franco.

Benea, L., Bonora, P.L., & Borello, A. (2002). Wear corrosion properties of nano-structured SiC-nickel composite coatings obtained by electroplat*ing, Wear,* 249, (10-11), 995.

Bohe, A.E., Vilche, J.R., Ju¨ttner, K., Lorenz, W.J., Kautek, W., & Paatasch, W. (1991). An electrochemical impedance spectroscopy study of passive zinc and low alloyed zinc electrodes in alkaline and neutral aqueous solutions, *Corros. Sci.*, 32, 621.

Chandrasekar, M.S., & Pushpavanam, M. (2009). Morphology and texture of pulse plated zinc–cobalt alloy, *Materials Chemistry and Physics,* 115, 603–611.

Chandrasekar, M.S., Pushpavanam, M. (2008). Pulse and pulse reverse plating-Conceptual, advantages and applications, *Electrochimica Acta*, 53, 3313–3322.

Chang, L., An, M., & Ma M. (2005). Investigation on microstructure and corrosion resistance of rare earth-doped electrodeposition Ni coatings, *J. Rare Earth*, 23, 456.

Changa, L.M., Chena, D., Liub, J.H., & Zhang, R.J. (2009). Effects of different plating modes on microstructure and corrosion resistance of Zn–Ni alloy coatings, *Journal of Alloys and Compounds*, 479, 489–493.

Ciubotariu, A. C., Benea, L., Lakatos, & M., Dragan, V. (2008). Electrochemical impedance spectroscopy and corrosion behavior of Al_20_3-Ni nano composite coatings, *Electrochimica Acta*, 53, 4557–4563.

Fan, Y., Zhang, Y., & Yang, X. (2004). Corrosion resistance of electrodeposited Zn-$FeSi0_2$ composite coatings. *Corros. Sci. & Prot. Technol.*, 16, (4), 245.

Garcia, I., Fransaer, J., & Celis, J.P. (2001). Electrodeposition and sliding wear resistance of nickel composite coatings containing micron and submicron SiC particles, *Surf. Coat. Technol.*, 148, 171-178.

Gavrila, M., Millet, J.P., & Mazille, H. (2000). Corrosion behaviour of zinc-nickel coatings electrodeposited on steel, *Surf. Coat. Technol.*, 123, (2-3), 164.

Hammami, O., Dhouibi, L., & Triki, E. (2009). Influence of Zn–Ni alloy electrodeposition techniques on the coating corrosion behaviour in chloride solution, *Surface & Coatings Technology*, 203, 2863–2870.

Hou, K.H., Ger, M.D., Wang, L.M., & Ke, S.T. (2002). The wear behaviour of electro-codeposited Ni–SiC composites, *Wear*, 253, 994–1003.

Kanani, N. (2004), *Electroplating- Basic Principles, Processes and Practice.* Berlin: Atotech Deutschland GmbH.

Kuo, S.L., Chen, Y.C., Ger, M.D., & Hwu, W.H. (2004). Nano-particles dispersion effect on Ni/Al_2O_3 composite coatings, *Mater. Chem. Phys.*, 86, (1) 5.

Lee, C.C., & Wan, C.C. (1988). A study of the composite electrodepition of copper with alumina powder, *Electrochem. Soc*., 135, (8), 1930.

Lehman, E. B., Ozga, P., Swiatek, Z. (2002). Electrodeposition of Zn-Ni protective coatings from sulfate-acetate baths, *Surf. Coat. Technol.*, 151-152.

Leighton, T.G. (1994). *The Acoustic Bubble*, Academic Press, New York.

Lekka, M., Kouloumbi, N., Gajo, M., & Bonora, P. L. (2005). Corrosion and wear resistant electrodeposited composite coatings, *Electrochimica Acta*, 50, 4551–4556.

Low, C.T.J., Wills, R.G.A., & Walsh, F.C. (2006). Electrodeposition of composite coating containing nanoparticles in a metal deposit, Surface & Coatings Technology, *201, 371–383.*

Luyck, S. & Love, A. (2004). The relationship between the abrasion resistance and the hardness of WC-Co alloys, *The Journal of The South African Institute of Mining and Metallurgy*, 223, 579-582.

Prime Minister's Science, Engineering and Innovation Council (PMSEIC). (2005). *Enabling technologies for Australian innovative industries*, Australia.

Qu, N.S., Chan, K.C., & Zhu, D. (2004). Pulse co-electrodeposition of nano Al_2O_3 whiskers nickel composite coating, *Scripta Mater.*, 50, (8) 1131–1134.

Ramanauskas, R., Quintana, P., Maldonado, L., Pome´s, R., & Pech-Canul, M.A. (1997). Corrosion resistance and microstructure of electrodeposited Zn and Zn alloy coatings, *Surface & Coatings Technology,* 92, 16-21.

Shrestha, N.K., Hamal, D.B., & Saji, T. (2004). Composite plating of Ni-P-Al_20_3 in two steps and its anti-wear performance. Surf. *Coat*. *Technol.*, 183, (2-3), 247.

Stroumbouli, M., Gyftou, P., Pavlatou, E.A., & Spyrellis, N. (2005). Codeposition of ultrafine WC particles in Ni matrix composite electrocoatings, *Surface & Coatings Technology*, 195, 325-332.

Thiemig, D., Cantaragiu, A.M., Schachschal, S., Bund, A., Pich, A., Carac, G., & Gheorghie, C. (2009). Electrocodeposition of hydroxyapatite nanoparticles with zinc–iron alloys, *Surface & Coatings Technology*, 203, 1488–1493.

Uzun, O., Kolemen, U., Celebi, S., & Guclu, N. (2005). *J. Eur. Ceram. Soc.*, 25, 969.

Vaskevich A. , Sinapi F., & Mekhalif Z. (2005). Underpotential deposition of nickel on {1111–textured gold electrodes in dimethyl sulfoxide, *J. Electrochem. Soc.*, 152, (11), 744.

Vilche, J.R., Ju¨ttner, K., Lorenz, W.J., Kautek, W., Paatsch, W., Dean, M.H., & Stimming, U. (1989). Semiconductor Properties of Passive Films on Zn, Zn-Co, and Zn-Ni Substrates, *J. Electrochem. Soc.*, 136, 3773.

Wilcox, G.D., & Gabe, D.R. (1993). Electrodeposited zinc alloy coatings. *Corros*. *Sci*., 35, *(5-8)*, 1251.

Wu, G., Li, N., Zhou, D. (2004). Electrodeposited Co-Ni-Al_2O_3 composite coatings, Surf. *Coat. Technol.*, 176, (2), 157.

Yang, F., Ma, Z., & Huang L. (2004). Electrodeposition, structure and properties of an amorphous Ni-W-B/$Zr0_2$ composite coating, *Acta Phys. Chim. Sin.*, 20, (12), 1411.